ISSN 2523-6849

Volume 7, Issue 17 – January – June – 2023

Journal of Physiotherapy and Medical Technology

ECORFAN®

Journal of Physiotherapy and Medical Technology, Volume 7, Issue 17, January-June 2023, is a journal published semi-annually by ECORFAN-Taiwan. Taiwan, Taipei. YongHe district, ZhongXin, Street 69. Postcode: 23445. WEB: www.ecorfan.org/taiwan, revista@ecorfan.org. Editor in Chief: IGLESIAS-SUAREZ, Fernando. MsC. ISSN: 2523-6849. Responsible for the last update of this issue of the ECORFAN Informatics Unit. ESCAMILLA-BOUCHÁN Imelda, LUNA-SOTO, Vladimir, updated June 30, 2023.

Journal of Physiotherapy and Medical Technology

Definition of Journal

Scientific Objectives

Support the international scientific community in its written production Science, Technology and Innovation in the Field of Medicine and Health Sciences, in Subdisciplines of surgery, physical exercise, physiotherapeutic treatment, thermotherapy, muscular physiology program, ultrasound, rehabilitation, augmented reality, articulated prosthesis.

ECORFAN-Mexico, S.C. is a Scientific and Technological Company in contribution to the Human Resource training focused on the continuity in the critical analysis of International Research and is attached to CONAHCYT-RENIECYT number 1702902, its commitment is to disseminate research and contributions of the International Scientific Community, academic institutions, agencies and entities of the public and private sectors and contribute to the linking of researchers who carry out scientific activities, technological developments and training of specialized human resources with governments, companies and social organizations.

Encourage the interlocution of the International Scientific Community with other Study Centers in Mexico and abroad and promote a wide incorporation of academics, specialists and researchers to the publication in Science Structures of Autonomous Universities - State Public Universities - Federal IES - Polytechnic Universities - Technological Universities - Federal Technological Institutes - Normal Schools - Decentralized Technological Institutes - Intercultural Universities - S & T Councils - CONAHCYT Research Centers.

Scope, Coverage and Audience

Journal of Physiotherapy and Medical Technology is a Journal edited by ECORFAN-Mexico, S.C. in its Holding with repository in Taiwan, is a scientific publication arbitrated and indexed with semester periods. It supports a wide range of contents that are evaluated by academic peers by the Double-Blind method, around subjects related to the theory and practice of surgery, physical exercise, physiotherapeutic treatment, thermotherapy, muscular physiology program, ultrasound, rehabilitation, augmented reality, articulated prosthesis with diverse approaches and perspectives , that contribute to the diffusion of the development of Science Technology and Innovation that allow the arguments related to the decision making and influence in the formulation of international policies in the Field of Medicine and Health Sciences. The editorial horizon of ECORFAN-Mexico® extends beyond the academy and integrates other segments of research and analysis outside the scope, as long as they meet the requirements of rigorous argumentative and scientific, as well as addressing issues of general and current interest of the International Scientific Society.

Editorial Board

Arbitration Committee

Assignment of Rights

The sending of an Article to Journal of Physiotherapy and Medical Technology emanates the commitment of the author not to submit it simultaneously to the consideration of other series publications for it must complement the Originality Format for its Article.

The authors sign the Authorization Format for their Article to be disseminated by means that ECORFAN-Mexico, S.C. In its Holding Taiwan considers pertinent for disclosure and diffusion of its Article its Rights of Work.

Declaration of Authorship

Indicate the Name of Author and Coauthors at most in the participation of the Article and indicate in extensive the Institutional Affiliation indicating the Department.

Identify the Name of Author and Coauthors at most with the CVU Scholarship Number-PNPC or SNI-CONAHCYT- Indicating the Researcher Level and their Google Scholar Profile to verify their Citation Level and H index.

Identify the Name of Author and Coauthors at most in the Science and Technology Profiles widely accepted by the International Scientific Community ORC ID - Researcher ID Thomson - arXiv Author ID - PubMed Author ID - Open ID respectively.

Indicate the contact for correspondence to the Author (Mail and Telephone) and indicate the Researcher who contributes as the first Author of the Article.

Plagiarism Detection

All Articles will be tested by plagiarism software PLAGSCAN if a plagiarism level is detected Positive will not be sent to arbitration and will be rescinded of the reception of the Article notifying the Authors responsible, claiming that academic plagiarism is criminalized in the Penal Code.

Arbitration Process

All Articles will be evaluated by academic peers by the Double Blind method, the Arbitration Approval is a requirement for the Editorial Board to make a final decision that will be final in all cases. MARVID® is a derivative brand of ECORFAN® specialized in providing the expert evaluators all of them with Doctorate degree and distinction of International Researchers in the respective Councils of Science and Technology the counterpart of CONAHCYT for the chapters of America-Europe-Asia- Africa and Oceania. The identification of the authorship should only appear on a first removable page, in order to ensure that the Arbitration process is anonymous and covers the following stages: Identification of the Journal with its author occupation rate - Identification of Authors and Coauthors - Detection of plagiarism PLAGSCAN - Review of Formats of Authorization and Originality-Allocation to the Editorial Board-Allocation of the pair of Expert Arbitrators-Notification of Arbitration -Declaration of observations to the Author-Verification of Article Modified for Editing-Publication.

Instructions for Scientific, Technological and Innovation Publication

Knowledge Area

The works must be unpublished and refer to topics of surgery, physical exercise, physiotherapeutic treatment, thermotherapy, muscular physiology program, ultrasound, rehabilitation, augmented reality, articulated prosthesis and other topics related to Medicine and Health Sciences.

Presentation of Content

As first article we present, *Vision system to obtain spatial coordinates in bony protuberances of the human body through ArUco markers*, by CARRILLO-HERNÁNDEZ, Didia, SALAS-GARCÍA, Francisco and GARCÍA-CERVANTES, Heraclio, with adscription in the Universidad Tecnológica de León, as second article we present, *Characterization of composite material specimens manufactured in 3D printing for the construction of a shoulder Rehabilitation Prototype*, by GUANDULAY-ALCÁZAR, Miguel Ángel, FERRER-ALMARAZ, Miguel Ángel, ORTIZ ROA, Arturo and FLORES BALDERAS, Juan Nicolás, with adscription in the Universidad Tecnológica del Suroeste de Guanajuato, as third article we present, *Design and manufacture of a forelimb prosthesis prototype for a dog*, by FIGUEROA-PEÑA, Ángel Rael, GONZALEZ-VIZCARRA, Benjamín, DELGADO-HERNANDEZ, Alberto and CASTAÑEDA, Ana María, with secondment at the Universidad Autónoma de Baja California, as last article we present, *Bioinformatic evaluation and in vivo study of Orlistat in acute cholestatic damage*, by ALDABA-MURUATO Liseth Rubí, MACÍAS-PÉREZ José Roberto, RODRIGUEZ-RODRIGUEZ, Angela and ALVARADO-SÁNCHEZ Brenda, on secondment at the Universidad Autónoma de San Luis Potosí.

Content

Article **Journal of Physiotherapy and Medical Technology**
June, 2023 Vol.7 No.17 1-5

Vision system to obtain spatial coordinates in bony protuberances of the human body through ArUco markers

Sistema de visión para obtener coordenadas espaciales en protuberancias óseas del cuerpo humano a través de marcadores ArUco

CARRILLO-HERNÁNDEZ, Didia†*, SALAS-GARCÍA, Francisco and GARCÍA-CERVANTES, Heraclio

Universidad Tecnológica de León - Cuerpo Académico de Bioingeniería

ID 1st Author: *Didia, Carrillo-Hernández* / **ORC ID:** 0000-0001-9989-5884, **Researcher ID Thomson:** ABF-4839-2020, **CVU CONAHCYT ID:** 936937

ID 1st Co-author: *Francisco, Salas-García* / **ORC ID:** 0009-0003-3017-3762, **Researcher ID Thomson:** IUO-8572-2023, **CVU CONACYT ID:** 1306184

ID 2nd Co-author: *Heraclio, García-Cervantes* / **ORC ID:** 0000-0002-4229-9229, **Researcher ID Thomson:** X-5622-2019, **CVU CONACYT ID:** 290829

DOI: 10.35429/JP.2023.17.7.1.5 Received March 10, 2023; Accepted June 30, 2023

Abstract

Actually, the vision systems have a great impact in technological innovation, since they represent the eyes of any device or machine, therefore the importance of this is paramount. On the other hand, in one of the branches of biomechanics studies are carried out to diagnose disorders in the gait cycle of patients, normally a physiotherapist performs specific exercises to determine if there is an abnormally during the gait cycle, however, the accuracy of the diagnosis can become uncertain if the physiotherapist has carried out several continuous studies and factors such as lighting of the place or eye fatigue cause alterations in its diagnosis, therefore, with the development of this project it is intended to make a vision system that, from markers positioned on bony protrusions on the lower part of the human body, get the spatial coordinates (X, Y and Z), information that adding a post processing would allow obtaining data such as angular movements, angular velocities and custom gait cycles, fundamental data in the development of prostheses, orthoses or exoskeletons, and considering that the project is carried out in free software, its implementation becomes more accessible.

Vision systems, Spatial coordinates, Python

Resumen

En la actualidad los sistemas de visión tienen un gran impacto en innovaciones tecnológicas, ya que representan los ojos de cualquier dispositivo o maquinaria, por lo tanto, la importancia de éste es primordial. Por otro lado, en una de las ramas de biomecánica se realizan estudios para diagnosticar padecimientos en el ciclo de marcha de las pacientes, normalmente un fisioterapeuta realiza ejercicios específicos para determinar si existe anormalidad en el ciclo de marcha, sin embargo, la precisión del diagnóstico puede llegar a ser poco certera si el fisioterapeuta ha realizado varios estudios continuos y factores cómo iluminación del lugar o fatiga ocular provocan alteraciones en su diagnóstico, por lo tanto, con el desarrollo de este proyecto se pretende realizar un sistema de visión qué, a partir de marcadores posicionados en protuberancias óseas de la parte inferior del cuerpo humano, se obtengan las coordenadas espaciales (X, Y y Z), información que agregando un post procesamiento permitiría obtener datos cómo movimientos angulares, velocidades angulares y ciclos de marcha personalizados, datos fundamentales en el desarrollo de prótesis, ortesis o exoesqueletos, y considerando que el proyecto está realizado en software libre, su implementación se vuelve más accesible.

Sistema de visión, Coordenadas espaciales, Python

Citation: CARRILLO-HERNÁNDEZ, Didia, SALAS-GARCÍA, Francisco and GARCÍA-CERVANTES, Heraclio. Vision system to obtain spatial coordinates in bony protuberances of the human body through ArUco markers. Journal of Physiotherapy and Medical Technology. 2023. 7-17: 1-5

* Correspondence to the Author (e-mail: dcarrillo@utleon.edu.mx)
† Researcher contributing as first author

Introduction

The study of the movement of the human body, as well as its causes, has been the subject of research throughout history in cultural, scientific or medical fields. Currently, there are areas such as bioengineering or biomedicine that require studies of the kinematics of the human body to solve different problems related to human gait, mainly due to vascular diseases that could cause transfemoral, knee, transtibial or ankle amputations; some other factors that alter the normal gait cycle are trauma, mainly the rupture of one or more bones, causing patients to require rehabilitation and special adaptations in their lower extremities to recover the greatest possible mobility [I-IV].

The boom in this area is so great that the number of laboratories and equipment that exist is not enough to meet the demand of patients who require these services, since it is known that annually in the country there are more than 27 thousand amputations and 80% of these are of lower limbs, it is also known that only 10% of patients receive a passive prosthetic equipment, On the other hand, existing vision systems such as VICON [IX], which is currently the most widely used due to its wide variety of applications, is a technology that most people cannot access due to its high cost.

There is another field of application of vision systems in the monitoring of the gait cycle, the area of sport, where, from the study of their physical abilities that the patient performs during their gait cycle, applied to activities such as cycling or walking, routines are diagnosed to strengthen their physical activity [IX].

The objective of this project was to obtain the spatial coordinates of specific points of the human body, mainly of bony protrusions, located from the hip to the feet, using computer vision, and developed in free software using a Perfect Choice PC-320494 camera, with the purpose of a post processing that would allow to obtain data how angular movements, angular speeds and personalized gait cycles, fundamental data in the development of prosthesis, orthosis or exoskeletons [X].

Methodology to be developed

The development of the vision system was with the intention of obtaining a technological innovation capable of extracting the movements of a patient's gait cycle through the monitoring of ArUco markers.

The programming was done in Python version 3.7 [XI], some libraries that were used are openpyxl, numpy, imutils, math, datetime, pathlib and OpenCV (opencv-contrib- python), in order to detect and process ArUco markers, these are mainly used in areas of augmented reality, their characteristics and the way of being processed were perfectly adapted to the needs that were presented.

The first procedure performed was the camera calibration, which is performed only once, the calibration algorithm requires at least 20 photographs with different view of the pattern shown in Fig.1, the photographs must be equal in dimensions (width and length).

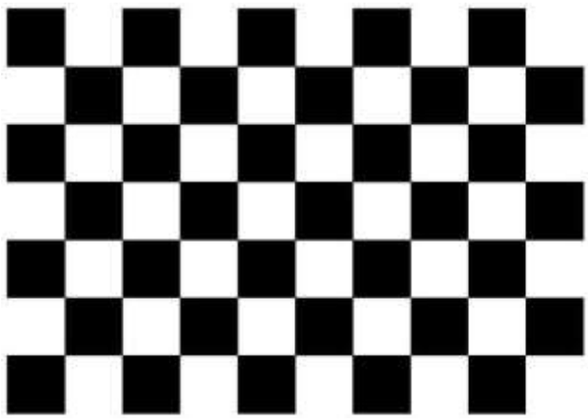

Figure 1 Calibration pattern

Aruco markers can be created with the function cv2.aruco.drawMarker of the OpenCV library, generating files with parameters such as: dictionary, Id, contour pixels and contour line. Additionally, there are sites on the Internet that allow to generate graphic markers and download them as PDF files.

To detect the markers in each frame we used the cv2 and cv2.aruco packages of the OpenCV library and a programmed function to save the parameters of the intrinsic matrix and distortion coefficients, followed by a conversion to grayscale of the frame. With these features the coordinates of the 4 corners of each marker are detected, as well as its id and objects rejected by the algorithm.

ISSN 2523-6849

The drawDetectedMarkers and drawAxis functions of the OpenCV library were used to visualize the markers on the screen. For the acquisition of coordinates the aruco.detectMarkers function was used, considering that the dimensions of the photographs with which the camera was calibrated are 5 times larger than the frames that make up the video, the value used for the size of the marker will be 2 (considering that each marker physically has a dimension of 10 x 10 cm).

The markers have different positions on the human body, mainly on the hip, sacrum, knees and ankles, to identify the body position the description of R (right), L (left), K (knee), A (ankle), H (hip) and SA (sacrum) were added, additional letters of JC were added to describe a kinematic joint, hence the acronym. Thus, if the acronym RKJC is described, it refers to the kinematic joint of the right knee.

Data storage was performed using math, datetime and openpyxl libraries, each record is made from a displacement greater than 7 pixels and was calculated using the Pythagorean theorem for a three-dimensional system.

Results

The vision system has the ability to detect up to 7 ArUco markers and draw a skeleton from given points.

1. Camera calibration

Figure 2 shows how the calibrate_chessboard function of the OpenCV library successfully finds the corners of the squares that make up the calibration pattern.

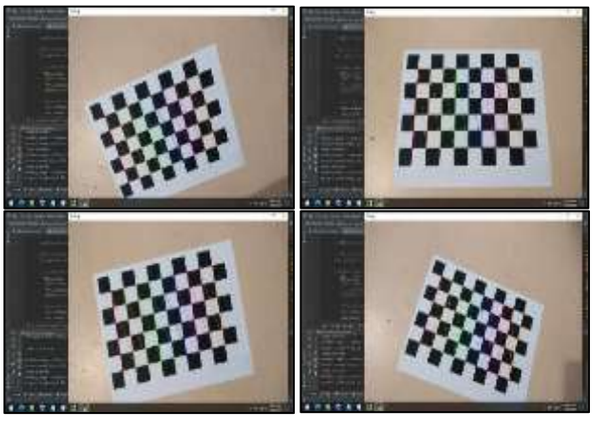

Figure 2 Calibrate_chessboard

This ensures that the intrinsic matrix calculation and distortion coefficients are calculated correctly.

2. ArUco markers

Seven markers were generated in PDF format from the web page https://chev.me/arucogen/, printed and adhered to a firm base to obtain better readings by the webcam. Fig. 3 shows some of the generated markers, ready for use with the mink system.

Figure 3 ArUco markers generated

3.- Detected Arc Markers

The program was able to calculate the orientation and position of each marker, being the illumination the only factor that produces erroneous values. In Fig.4 it can be seen that in the center of each marker a spatial coordinate axis is drawn, describing in order the colors red, green and blue, representing the X, Y and Z axes respectively.

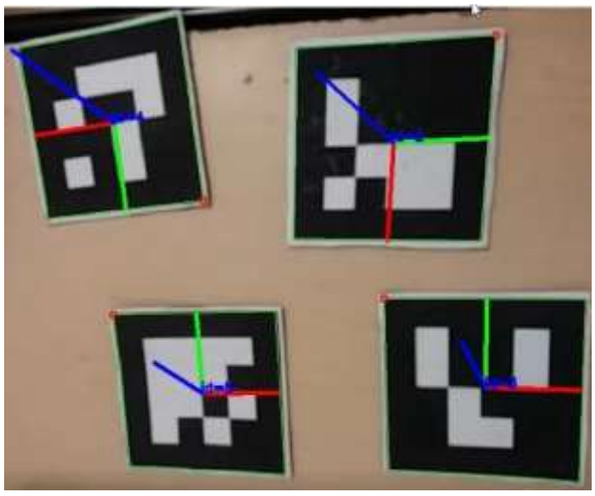

Figure 4 Coordinate axes on ArUco markers

ISSN 2523-6849

4. Acquisition of coordinates of ArUco markers

In addition to the generation of coordinate axes, the mimic system identifies each marker by ID and attributes a description to it in order to identify the position on the human body where it is located and draw the skeleton, as shown in Fig. 5.

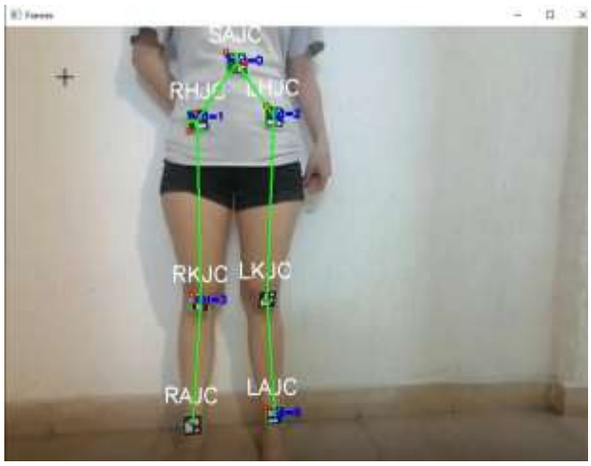

Figure 5 Skeleton drawn from the markers Arc

To corroborate the data obtained for the z coordinate, tests were performed to check the real distance with the value obtained in the vision system. The results showed a 3% error with respect to the real value in the z coordinate.

5.- Coordinate Storage in Excel

The storage was done individually, that is, for each different marker a new sheet was added in the Excel file, the data that were saved for each marker are: Id, Date, X, Y and Z coordinates, as shown in Fig.6.

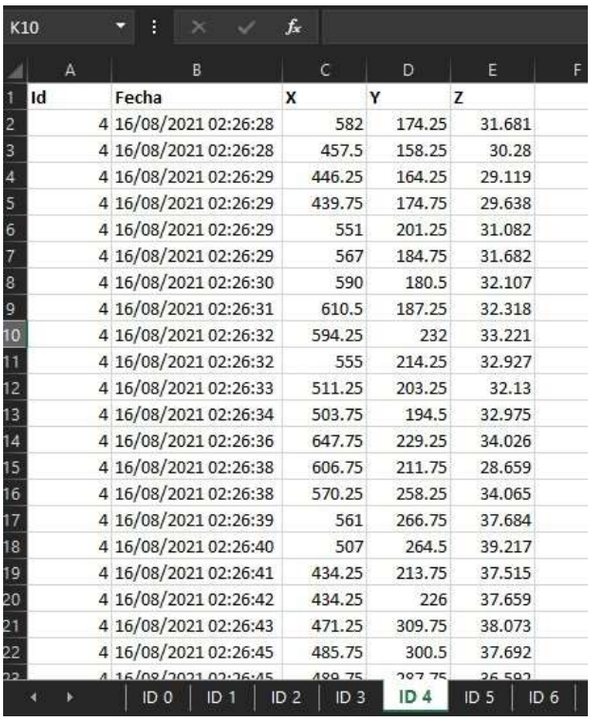

K10

	A	B	C	D	E	F
1	Id	Fecha	X	Y	Z	
2	4	16/08/2021 02:26:28	582	174.25	31.681	
3	4	16/08/2021 02:26:28	457.5	158.25	30.28	
4	4	16/08/2021 02:26:29	446.25	164.25	29.119	
5	4	16/08/2021 02:26:29	439.75	174.75	29.638	
6	4	16/08/2021 02:26:29	551	201.25	31.082	
7	4	16/08/2021 02:26:29	567	184.75	31.682	
8	4	16/08/2021 02:26:30	590	180.5	32.107	
9	4	16/08/2021 02:26:31	610.5	187.25	32.318	
10	4	16/08/2021 02:26:32	594.25	232	33.221	
11	4	16/08/2021 02:26:32	555	214.25	32.927	
12	4	16/08/2021 02:26:33	511.25	203.25	32.13	
13	4	16/08/2021 02:26:34	503.75	194.5	32.975	
14	4	16/08/2021 02:26:36	647.75	229.25	34.026	
15	4	16/08/2021 02:26:38	606.75	211.75	28.659	
16	4	16/08/2021 02:26:38	570.25	258.25	34.065	
17	4	16/08/2021 02:26:39	561	266.75	37.684	
18	4	16/08/2021 02:26:40	507	264.5	39.217	
19	4	16/08/2021 02:26:41	434.25	213.75	37.515	
20	4	16/08/2021 02:26:42	434.25	226	37.659	
21	4	16/08/2021 02:26:43	471.25	309.75	38.073	
22	4	16/08/2021 02:26:45	485.75	300.5	37.692	

ID 0 | ID 1 | ID 2 | ID 3 | ID 4 | ID 5 | ID 6

Figure 6 Excel file with essential information of each ArUco marker

Acknowledgements

We would like to thank the Universidad Tecnológica de León for allowing the development of this type of project, providing the necessary time and equipment; we would also like to thank the collaborators and all those involved for their great effort and time invested.

Conclusions

The use of the OpenCV library was undoubtedly the best option for image and video processing, since excellent results were obtained without affecting the performance of the equipment. On the other hand, the ArUco markers allowed to facilitate the detection of specific points because they are easily recognizable in an image regardless of the background or the environment in which they are located, and their features such as having a unique identifier (id) or the facility they provide to locate them in a three-dimensional space with a single camera were perfectly adapted to the needs of the project.

ISSN 2523-6849

Although it was necessary to have good lighting, a good camera and to keep the markers fully extended during motion capture, using ArUco marks to identify the various points of the human body presented a great advantage over the other options that were considered, since other identifiers based on color or shapes were highly limited by the environment.

Finally, it is necessary to emphasize that the three-dimensional coordinates obtained for each marker from a two-dimensional system are accurate as long as the appropriate environmental conditions are present.

Although the current software has much room for improvement, the way has been marked for its correction, implementation and possible future expansion.

References

[I] Herr, H. (2009). Exoskeletons and orthoses: Classification, design challenges and future directions. *Journal of NeuroEngineering and Rehabilitation*, *6*(1), 1–9. https://doi.org/10.1186/1743-0003-6-21

[II] Hugh, H. M., & Villalpando, E. (2011). *Innovación: cambiar el rostro de la discapacidad OpenMind*. https://www.bbvaopenmind.com/articul os/innovacion-cambiar-el-rostro-de-la-discapacidad/

[III] Martín Nogueras, A., Calvo Arenillas, J. L., Orejuela Rodríguez, J., Barbero Iglesias, F. J., & Sánchez Sánchez, C. (2019). Fases de la marcha humana. *Revista Iberoamericana de Fisioterapia y Kinesiología*, 1–11. https://www.elsevier.es/es-revista- revista-iberoamericana-fisioterapia- kinesiologia-176-articulo-fases-marcha- humana-13012714

[IV] Organización Mundial de la Salud. (2011). Informe mundial sobre la discapacidad. *Informe Mundial Sobre la discapacidad*, 388. http://www.who.int/disabilities/world_report/20 11/report/en/

[V] Neumann, E. S. (2009). State of the Science Review of Transtibial Prosthesis Alignment Pertubation. *Journal of Prosthetics and Orthotics*. DOI:10.1097/JPO.0b013e3181baaa68

[VI] Vázquez Vela, E. (2016). Los amputados y su rehabilitación. Un reto para el Estado. *Academia Nacional de Medicina de México*, 162. https://www.anmm.org.mx/publicacione s/ultimas_publicaciones/Rehabilitacion.pdf#pag e=144%0Ahttps://www.anmm.org.mx/publicaci ones/ultimas_publicaciones/Rehabilitacion.pdf

[VII] Vazquez Vela, E., Hijar Medina, M., L, R. P., Espinosa Jove, I. G., & Rojas, X. (2015). Los amputados, un reto para el Estado. *Acta de la Sesión del 4 de marzo del 2015 Academia Nacional de Medicina*, 9. https://doi.org/10.1017/CBO9781107415324.00 4

[VIII] Villarejo, J., Caicedo, E., & Campo, O. (2008). Detección de la intención de movimiento durante la marcha a partir de señales electromiográficas. *Universidades del valle y autónoma de occidente*, *1*, 1–7. http://hdl.handle.net/10893/1487

[IX] Systems, V. M. (s/f). *VICON*. https://www.vicon.com/about-us/what- is-motion-capture/

[X] Carrillo-Hernández, D., Terrones-Lara, Y. U., García-Cervantes, H., & Blanco- Miranda, A. D. (2020). Diseño de interfaz gráfica para analizar el ciclo de marcha del cuerpo humano en software libre. *Revista de Ingeniería Biomédica y Biotecnología*, *4*(12), 13–17. https://doi.org/10.35429/jbeb.2020.12.4.13.17

[XI] Rossum, G. van. (s/f). *Python*. https://www.python.org/about/gettingstar ted/

ISSN 2523-6849

Article **Journal of Physiotherapy and Medical Technology**
June, 2023 Vol.7 No.17 6-11

Characterization of composite material specimens manufactured in 3D printing for the construction of a shoulder Rehabilitation Prototype

Caracterización de probetas de material compuesto fabricadas en impresión 3D para construcción de prototipo rehabilitador de hombro

GUANDULAY-ALCÁZAR, Miguel Ángel, FERRER-ALMARAZ, Miguel Ángel, ORTIZ ROA, Arturo and FLORES BALDERAS, Juan Nicolás

Universidad Tecnológica del Suroeste de Guanajuato

ID 1st Author: *Miguel, Guandulay-Alcázar* / **ORC ID**: 0000-0002-8831-9547, **Researcher ID Thomson**: S-6750-2018, **CVU CONAHCYT ID**: 443671

ID 1st Co-author: *Miguel, Ferrer -Almaraz* / **ORC ID**: 0000-0003-4913-4010, **Researcher ID Thomson**: S-6969-2018, **CVU CONAHCYT ID**: 342076

ID 2nd Co-author: *Arturo, Ortiz-Roa* / **ORC ID**: 0000-0003-0543-7810, **Researcher ID Thomson**: S-7642-2018, **CVU CONAHCYT ID**: 947387

ID 3rd Co-author: *Juan, Flores-Balderas* / **ORC ID**: 0000-0002-3097-7504, **Researcher-ID Thomson**: IQW-2569-2023, **CVU CONAHCYT ID**: 632361

DOI: 10.35429/JP.2023.17.7.6.11 Received March 10, 2023; Accepted June 30, 2023

Abstract

The present work seeks to characterize polymer specimens with aluminum and stainless steel reinforcements, using additive manufacturing for their elaboration and thus increase their tensile strength and implement them for industrial, medical and automotive use. The methodology to follow consists of a documentary investigation of related articles and standards such as ASTM D638, where the tensile properties of plastics are specified, continuing with the manufacture of the test tubes in a 3D printer, this according to the corresponding standard., to later carry out stress tests on the universal machine. The contribution of the work developed lies in the increase in the tensile strength of the composite material experienced, resulting for a first test tube an increase of 52.4% in the maximum tensile strength with an aluminum reinforcement, and an increase of 59.1%, this with a steel reinforcement, in the second specimen submitted to tests with aluminum reinforcement an increase of 20.04% was obtained and with the steel reinforcement it was 84.54%.

Test Tube, Polymer, 3D

Resumen

El presente trabajo busca caracterizar probetas de un polímero con refuerzos de aluminio y acero inoxidable, utilizando manufactura aditiva para su elaboración y así aumentar su resistencia a la tensión e implementarlas para uso industrial, médico y automotriz. La metodología a seguir consiste en una investigación documental de artículos relacionados y normas como la ASTM D638, donde se específica las propiedades a la tracción de los plásticos, continuando con la fabricación de las probetas en una impresora 3D, esto de acuerdo a la norma correspondiente, para posteriormente efectuar pruebas de tensión en la máquina universal. La contribución del trabajo desarrollado radica en el aumento de la resistencia a la tracción del material compuesto experimentado resultando para una primera probeta un incremento del 52.4% en la resistencia a la tracción máxima con un refuerzo de aluminio, y un incremento del 59.1%, esto con un refuerzo de acero, en la segunda probeta sometida a pruebas con refuerzo de aluminio se obtuvo un incremento de 20.04% y con el refuerzo de acero fue 84.54%.

Probeta, Polímero, 3D

Citation: GUANDULAY-ALCÁZAR, Miguel Ángel, FERRER-ALMARAZ, Miguel Ángel, ORTIZ ROA, Arturo and FLORES BALDERAS, Juan Nicolás. Characterization of composite material specimens manufactured in 3D printing for the construction of a shoulder Rehabilitation Prototype. Journal of Physiotherapy and Medical Technology. 2023. 7-17: 6-11

* Correspondence to the Author (e-mail: maguandulay@utsoe.edu.mx)
† Researcher contributing as first author

Introduction

The process to carry out the additive manufacturing starts with the geometric modeling of the part in space, using some computer aided design software, such as SolidWorks, then a conversion of the dimensioned model to a coded reading of G commands will be done, that is to establish the necessary instructions to manufacture the part, then by means of a communication system the information is transferred to a processor that generates the additive manufacturing by joining the material layer by layer. The economic reduction of resources and manufacturing time are points in favor of additive manufacturing. The diverse applications that additive manufacturing has nowadays force to develop suitable materials that can give solution to the problems posed by the industry, such as the improvement of the mechanical properties of the same, such as yield strength or tensile strength, the use of bio-based materials is significant.

For example, the use of bioplastic materials, such as PLA or a polymer such as ABS, used in food applications, or in the manufacture of gears, is significant, being in this way the problem to be solved: to have available parts made of a molten polymer material, manufactured by means of a 3D printer, these parts would have to have a tensile strength or ultimate, close to steel or aluminum to be used industrially, for this steel and aluminum materials will be added to the materials already mentioned resulting in a composite material whose mechanical properties should be significantly improved. In addition, additive manufacturing is standardized by ISO/ASTM 52900 [5], which establishes the manufacture of components with 3D printers, in general.

Development

In the realization of the present experimental experimental a PLA (polylactic acid) polymer material will be used, as well as ABS resin in filament form, this due to its malleability and low cost, the ultimate strength of the PLA thermoplastic polymer is between 40 and 60 MPa [2], while the ABS material has a tensile strength between 41 and 45 MPa [3].

The solution to the above problem is to generate a composite material consisting of PLA and ABS, in addition to the addition of other materials, respectively, and to add other materials [4] other materials respectively,

The materials to be added will be: stainless steel and aluminum, due to their cost and accessibility, all of which should improve the mechanical properties of the base material. The materials to be added will be: stainless steel AISI 302, cold rolled, whose tensile strength or ultimate strength is 860 MPa and for aluminum 6061-T6 is 260 MPa [1].

1. Tensile test

In order to perform the tensile test, a specimen will be used A specimen will be used, according to ASTM D638 [4], called: Standardized Test Method for Tensile Properties of Plastics. The specifications of the standardized specimen to perform the tensile tests are shown in Figure 1. The specimens used by this standard are classified by types, as described below.

Type I

Type I specimen is preferably used, and should be used when there is sufficient material with a thickness of 7 mm (0.28 in.).

Type II

This specimen is recommended when the breakage of type I does not occur in its narrow part.

Type III

Type III specimen should be used for all materials with a thickness greater than 7 mm (0.28 in.) but not greater than 14 mm (0.55 in.). In this case, both the width of the narrow parallel section and the head width and overall length are increased so that the specimen thickness is less than the width.

Type IV

Generally used when direct comparisons between materials in different stiffness cases (i.e. non-rigid and semi-rigid) are required.

ISSN 2523-6849

Type V

If only a small amount of material is available, or if it is not possible to extract a larger specimen from a component, then a type V specimen is used, reduced in all its dimensions with respect to type I. It can be stainless steel and aluminum, this due to its cost and accessibility, all of which should improve the mechanical properties of the base material. The materials to be added will be: stainless steel AISI 302, cold rolled, whose tensile strength or ultimate strength is 860 MPa and for aluminum 6061-T6 is 260 MPa [1].

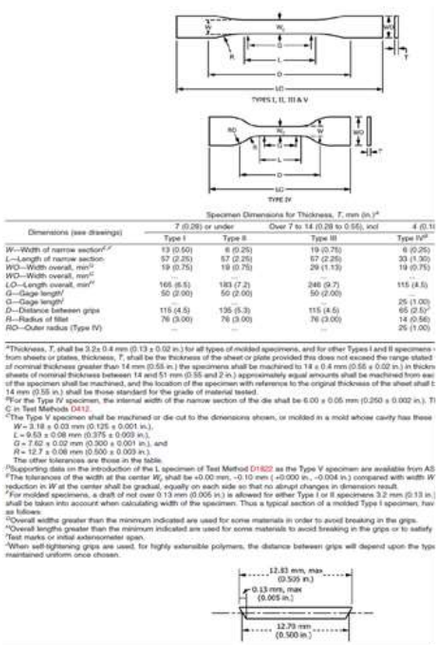

Figure 1 Specifications for standardized specimen, tensile test [4]

2. Additive manufacturing process of the specimens

The specimens were modeled in SolidWorks software, according to the parameters of the type I specimen, with a thickness of 7 mm and 165 mm total length, as well as 13 mm width in the narrowest section and a bending radius of 76 mm. Type I specimens will be manufactured in ABS material and type II in PLA material, the generated designs are saved with STL extension so that in the Digilab 3D Slicer software is converted into a control file for the 3D printer, this file is composed and is called G-Code consisting of G and M commands each with a movement or action assigned, Figure 2 shows an example of the G-Code of one of the specimens manufactured in 3D.

With the combination of these, transformed into a programming language that allows the 3D printer to understand which commands must be executed so that the part can be printed by the layer-by-layer process.

```
M140 S60
M104 S230
M109 S230
G28
G1 Z50.00 F400
G92 E0
G1 F200 E3
G92 E0
M132 X Y Z A
M907 X100 Y100 Z50 A100
;LAYER_COUNT:16
;LAYER:0
M107
M204 S2000
G0 F3000 X-17.671 Y11.3 Z0.3
;TYPE:SKIRT
G1 F1500 X-23.113 Y11.454 E0.27161
G1 X-28.486 Y11.911 E0.54064
G1 X-33.825 Y12.672 E0.8097
G1 X-41.55 Y14.195 E1.20252
G1 X-42.164 Y14.276 E1.23341
G1 X-42.479 Y14.286 E1.24914
```

Figure 1 G-Code sample from one of the specimens

In this same software the additive manufacturing parameters are specified, as described below:

Printing material

PLA and ABS with a diameter of 1.75mm.

Quality

The quality is related to the layer height, higher values produce a faster print with a lower resolution and lower values produce a slower print with a higher resolution, in this case a quality of 0.2 mm was used, the highest and lowest value handled by the DREMEL 3D 45 printer is 0.3 and 0.05 mm respectively.

ISSN 2523-6849

Filling

Adjusts the density for the printing filling, a 100% filling was used, this makes the printed model completely solid, the lower this percentage, the lower the resistance of the material.

Printing temperatura

The printing temperature of the PLA filament, extruder nozzle of 220 °C and the printing bed of 30 °C, for the ABS filament it was 240 °C and 60 °C respectively.

Speed and acceleration

Printing speed was 60 mm/s, displacement speed was 120 mm/s, printing acceleration was 2000 mm/s2 and displacement acceleration was 5000 mm/s2.

Once all the above parameters are defined, Digilab 3D Slicer generates the G-code, which is the programming language used.

The printing of the ABS and PLA specimens, Figure 3, was performed on a DREMEL 3D45 printer, it has a build volume of 9x9.9x5.5 inches (230x150x140mm) with a layer thickness of 50 µm. Type I samples were printed with ABS material and type II with PLA material.

Figure 3 3D printed PLA test tube

3. Implementation of reinforcement to the type I specimen

After the fused deposition modeling (MDF) process of the specimens, the reinforcement was implemented to the specimen, the material used for the reinforcement was aluminum and steel independently, Figure 4. The aluminum and steel sheets were cut with the same dimensions as the 3D printed specimens.

Figure 4 ABS test tube with reinforcement material (aluminum)

4. Tensile tests for the analysis and interpretation of results

Once the specimens were obtained, the tensile tests were performed with a universal machine, the ABS type I specimens were fractured outside the narrowest part of the specimen, see Figure 5, in this case it is recommended to use the type II specimen according to ASTM D638 standard to obtain the most accurate results of the material strength.

Figure 5 Tensile test on a type I specimen, made of ABS material

ISSN 2523-6849

Since the fracture of the specimen type I was not in the middle part as recommended by the standard, the PLA specimens, type II, were used, in the same way they were reinforced with aluminum and steel independently, using the same process with the specimens reinforced with ABS, type I, to later perform the tension test in the universal machine, figure 6.

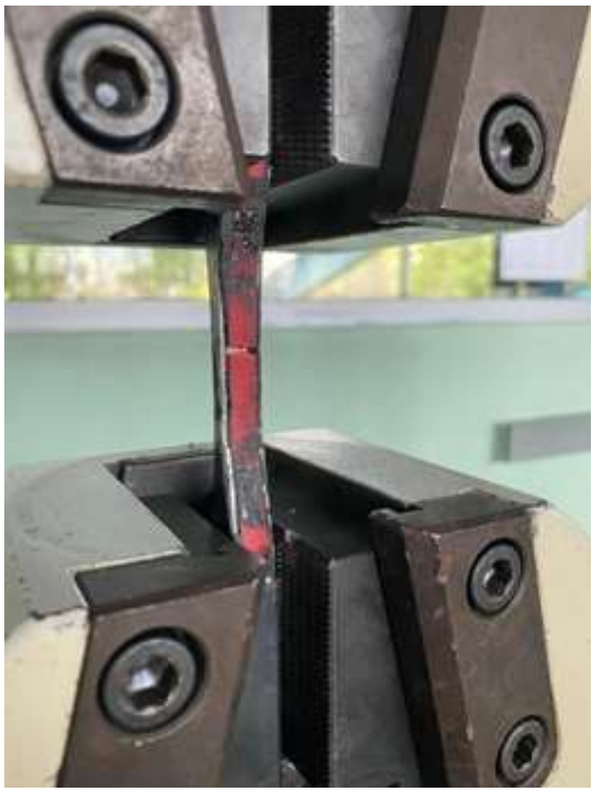

Figure 6 Tensile test on a type II specimen made of PLA material and reinforced with steel

The tests performed for the ABS material type I and PLA material type II specimens were three for each of them, the first was the original specimen without reinforcements, the second was with aluminum reinforcement and the last one with steel reinforcement, in total there were 6 tests, for each of these samples different results were obtained in relation to the tensile strength, i.e. each of them supports different loads, this was to be expected due to the mechanical properties of each material used in the printing of the specimens and the materials used in the reinforcements.

5. Results

As a result of the tensile tests carried out on the specimens manufactured with PLA and ABS both without reinforcement and with Alumina and steel reinforcement respectively, the values obtained are shown below:

Type of test tube	Material	Reinforcement	Tensile Strength, MPa
I	ABS	None	40.6
		Aluminum	61.9
		Steel	64.9
II	PLA	None	41.4
		Aluminum	49.7
		Steel	76.4

Table 1 Tensile test results, type I and II test specimens

6. Conclusions

The results obtained from the tensile tests carried out on ABS and PLA materials with aluminum and steel reinforcements, respectively, show an increase of 34.4% in tensile strength in the case of the ABS specimen with added aluminum and 37.4% increase with added steel % increase in the tensile strength in the case of the ABS specimen with added aluminum, 37.4 % increase with added steel, so the improvements are highly significant. With respect to the PLA material, the addition of aluminum increased the tensile strength by 9.16% and 45.8% with the addition of steel. All of the above is gratifying in the sense of the improvement of the conditions in the properties of the proposed materials, however, the costs of the additional materials to the base material must be considered, which could be a factor in deciding the material to be used.

This can be visualized in the future in a new study that would complement the present one.

This study proves and opens the opportunity to expand the area of application of these composite materials as mechanical elements where they will be subjected to tension or compression forces, as a very particular example in the development of projects focused on the field of bio-mechanics and physiotherapy, in the case of the latter, as future work is contemplated to develop a shoulder rehabilitator prototype, with composite material, having a great advantage in terms of cost and weight, this will make the project competitive and innovative.

7. References

[1] Beer, F. P. (2010). Mecánica de Materiales (5a. ed.). México: McGraw-Hill Interamericana.

ISSN 2523-6849

[2] Serna C. L, Rodríguez de S. A, Albán A. F. Ácido Poliláctico (PLA): Propiedades y Aplicaciones. inycomp [Internet]. 4 de junio de 2011 [citado 23 de mayo de 2023];5(1):16-2. Disponible en: https://revistaingenieria.univalle.edu.co/index.php/ingenieria_y_competitividad/article/view/2301

[3] Vargas-Henríquez, Lisandro. (2020). Caracterización del ABS utilizado en procesos de manufactura aditiva y el ABS natural. Scientia et Technica. [citado 23 de mayo de 2023];5(1):16-2. Disponible en: https://www.researchgate.net/publication/346254982_Caracterizacion_del_ABS_utilizado_en_procesos_de_manufactura_aditiva_y_el_ABS_natural

[4] ASTM International, ASTM D638-14 Standard test method for tensile properties of plastics (2015).

[5] ISO/ASTM, Additive Manufacturing - General Principies Terminology (ASTM52900), 2015. https://www.iso.org/standard/69669.html

[6] Y. A. Jin, J. Plott, R. Chen, J. Wensman, and A. Shih, "Additive manufacturing of custom orthoses and prostheses - A review," in Procedia CIRP, 2015, vol.36, pp. 199–204 doi: 10.1016/j.procir.2015.02.125.

[7] D. S. Chae *et al.*, "The functional effect of 3D-printing individualized orthosis for patients with peripheral nerve injuries: Three case reports," Medicine, vol. 99, no. 16, p. e19791, Apr. 2020, doi:10.1097/MD.0000000000019791.

[8] S. Janzen, K. Stewart, and P. P. Pott, "Low-cost active knee orthoses - A systematic evaluation: Assisted stair climbing and sit-to-stand," Current Directions in Biomedical Engineering, vol. 4, no. 1, pp. 649–652, Sep. 2018, doi: 10.1515/cdbme-2018-0156.

ISSN 2523-6849

Article **Journal of Physiotherapy and Medical Technology**
June, 2023 Vol.7 No.17 12-20

Design and manufacture of a forelimb prosthesis prototype for a dog

Diseño y manufactura de prototipo para prótesis de extremidad anterior para un can

FIGUEROA-PEÑA, Ángel Rael†*, GONZALEZ-VIZCARRA, Benjamín, DELGADO-HERNANDEZ, Alberto and CASTAÑEDA, Ana María

Universidad Autónoma de Baja California

ID 1st Author: *Ángel Rael, Figueroa-Peña* / **ORC ID**: 0009-0001-3008-4167

ID 1st co-author: *Benjamín, González-Vizcarra* / **ORC ID**: 0000-0003-2143-8725, **CVU CONAHCYT ID**: 101772

ID 2nd co-author: *Alberto, Delgado-Hernández* / **ORC ID**: 0000-0003-2132-9377, **CVU CONAHCYT ID**: 989649

ID 3rd co-author: *Ana María, Castañeda* / **ORC ID**: 0000-0003-2777-1107, **CVU CONAHCYT ID**: 268050

DOI: 10.35429/JP.2023.17.7.12.20 Received March 10, 2023; Accepted June 30, 2023

Abstract

The objective of this writing is to develop a methodology for the design and selection of materials that allows for the manufacturing of a canine prosthesis prototype based on anthropometric measurements, element simulation, and finite analysis. The canine prosthesis aims to restore mobility to a missing limb of a dog due to amputation and/or congenital malformation. The methodological approach for this study has been determined based on the analysis of a series of parameters, such as the dimensions of the animal leg, as well as its weight and the location of the amputation, to mention just a few points. As a contribution, a prototype of an exoprosthesis is proposed for a missing front limb, where it should fit within the range of the leg length, from 35 cm to 45 cm, and its weight should range between 30 kg and 40 kg. Additionally, the amputation should be located starting from the elbow region, and the optimal design should be able to adapt to different anthropometric measurements and the needs of the dogs.

Design, Prosthesis, Amputation

Resumen

El objetivo de este escrito es desarrollar una metodología para el diseño y selección de material que permita la manufactura de un prototipo de prótesis canina a partir de mediciones antropométricas, simulación de elementos y análisis finito. La prótesis canina permite restablecer la movilidad de una extremidad faltante de un can debido a una amputación y/o malformación congénita. El enfoque metodológico para este estudio se ha determinado en base al análisis de una serie de parámetros como son las dimensiones de la pata del animal, así como su peso y la localización de su amputación solo por mencionar algunos puntos. Como contribución se propone un prototipo de una exoprótesis para una extremidad faltante anterior, en donde este ocupe estar dentro del rango del largo de su pata de 35cm a 45 cm y su peso deberá oscilar entre los 30 kg a 40 kg, aparte su amputación debe localizarse a partir de la región del codo, con un diseño óptimo pueda adaptar a las diferentes medidas antropométricas y necesidades de los canes.

Diseño, Prótesis, Amputación

Citation: FIGUEROA-PEÑA, Ángel Rael, GONZALEZ-VIZCARRA, Benjamín, DELGADO-HERNANDEZ, Alberto and CASTAÑEDA, Ana María. Design and Manufacture of a Forelimb Prosthesis Prototype for a Dog. Journal of Physiotherapy and Medical Technology. 2023. 7-17: 12-20

* Correspondence to the Author (e-mail: rael.figueroa@uabc.edu.mx)
† Researcher contributing as first author

Introduction

Prosthesis

A prosthesis is an artificial substitute for a missing body part (both singular and plural; it is called a prosthesis). Physical and activity limits are the most important changes to cope with after amputation of part or all of a limb. The type of prosthesis that may be needed after surgery depends on the type and location of the amputation and how the limb has been left, any additional treatment that may be needed, the patient's lifestyle and needs.

For prostheses we have that these are broken down into two main types which are endoprosthesis and exoprosthesis (Prosthesis, 2020).

The basic components of a lower limb prosthesis and are shown in Figure 1 and these are (Alguacil *et al*., 2019):

– End devices, they refer to how the devices work.
– And what users can do with them e.g. Prosthetic foot.
– Intermediate elements: knees/hips.
– Prosthetic sockets and fittings (different depending on the level of amputation).
– Suspension systems and interfaces.
– Structures.

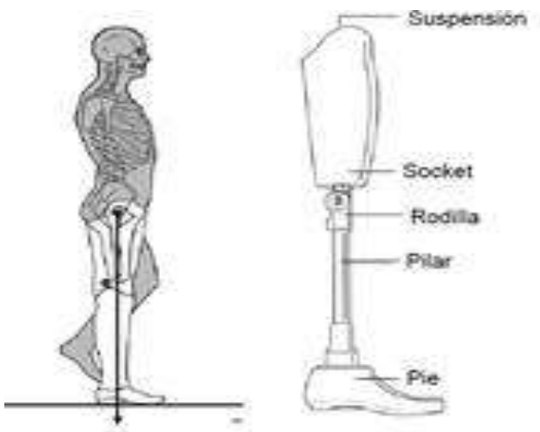

Figure 1 Components of a leg prosthesis
(Jaramillo, 2014)

Prostheses in canines

There are many variables as to why canines have their legs amputated, some of the main reasons are accidents, injuries or diseases that induce requiring the amputation of a leg, or a canine may have a congenital birth defect and is born without one of its legs. Many animals are able to adapt to a tripod or even bipedal life or any other condition they may have without any problem, this does not mean that their conditions are no longer a limitation.

The forelimbs in dogs receive the thrust, while the hind limbs are the most important since they handle resistance, thrust, trotting and stability. The use of prosthesis in one or more limbs provides dogs with a better quality of life, giving a solution to the motor problem, which implies physical limitations or injuries (Zavaleta, 2020). (Zavaleta, 2020)

a) b)

Figure 2 a) Prosthetic forelimb and b) prosthetic canine hind limbs
(Montano, 2022)

Manufacturing

Various materials are used in the manufacture of prostheses, e.g. thermosetting polyurethane. For pigmenting, resin dyes in paste or liquid form are used; for hip or knee joints, metals such as steel or titanium are often used. That is why different manufacturing processes can vary some examples are:

– By molding composite materials.

Figure 3 Manual fabrication of prosthesis with mold *(Hernandez et al., 2018)*

ISSN 2523-6849

– By machining

Figure 4 Grinding of prosthesis
(Metalmecánica, 2019)

– By alternative methods

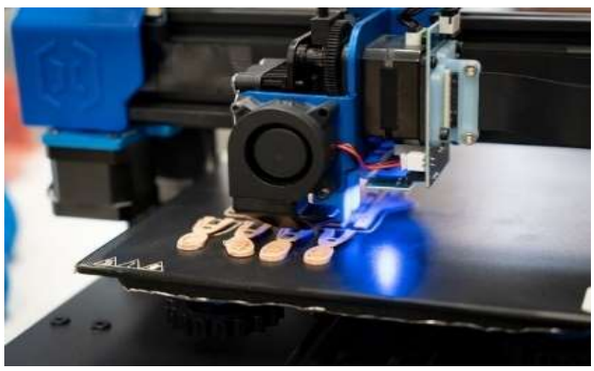

Figure 5 3D printing of prostheses
(Roldan, 2022)

Materials

Over the years different types of materials have been implemented at the time of the manufacture of prostheses going from the simplest to the most complex since due to the fact that with the passing of the years the need for the functionality of the prostheses has been increasingly demanding therefore better quality materials are required some of the main materials for the manufacture of orthopedic prostheses are:

– Woods, although these are no longer used today.
– Polymers, whether plastics, silicones, resins, polyurethanes, etc.
– Metals of different types of alloys.
– Ceramics (Galli & Pelozo, 2017), (Cely,2011).

Stress

Stress is defined as force per unit area in psi or MPa units. In an element subjected to certain forces, the stress is usually distributed as a constantly varying function within the continuum of the material. Each infinitesimal element of the material may experience different stresses at the same time. Therefore, the stresses acting on small evanescent elements within the part must be visualized as shown in Figure 6. (Norton,2011), (Beer & Johnston, 2010)

Figure 6 Stresses a) applied, b) normal and c) shear
(Norton, 2011)

2. Sketch

To start with the development of the prosthesis prototype design, we started with the sketches since it is the materialization of the ideas landed in a drawing, the considerations of the previous sections were taken into account for the prosthesis that will consist of four elements, a socket formed by a sleeve and strap, an intermediate element that will consist of a tube that will give the support and a terminal element that will be an arch that will function as a leg that will be attached to the connecting tube by means of a bolt; the sketches were made to comply with what has already been proposed.

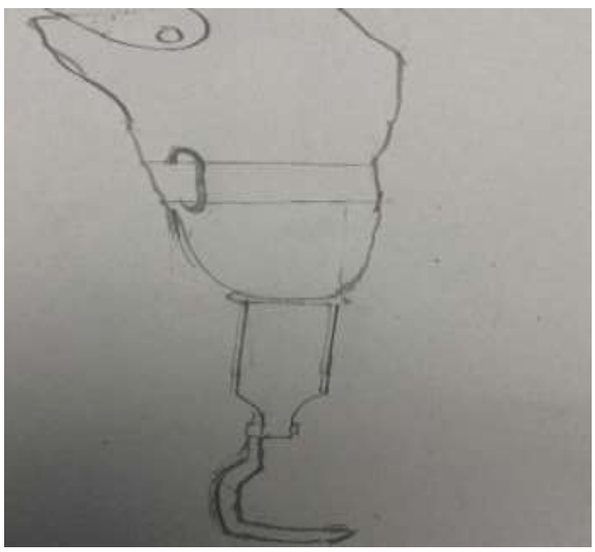

Figure 7 Prosthesis sketch

ISSN 2523-6849

3. Drawings

Following the sketch, the drawings of the different components of the prosthesis were made in SolidWorks in order to take into account their dimensions; it is worth mentioning that only the drawings of the components that will be subjected to important efforts were made.

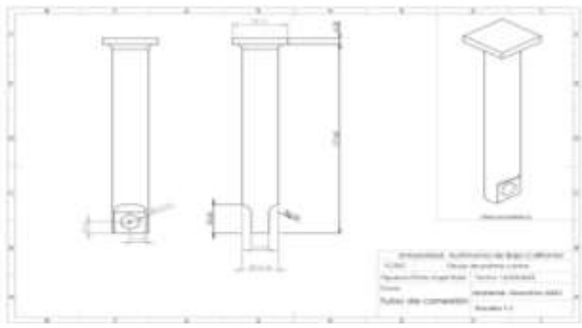

Figure 8 Drawings of the connection tuve

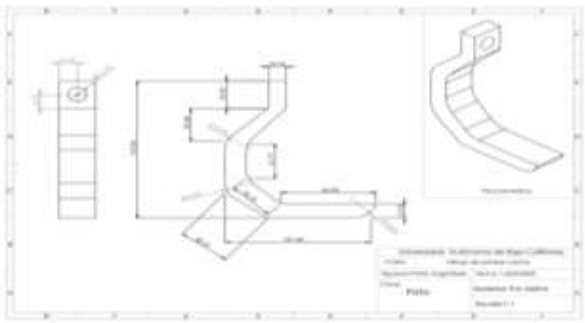

Figure 9 Drawings of the leg

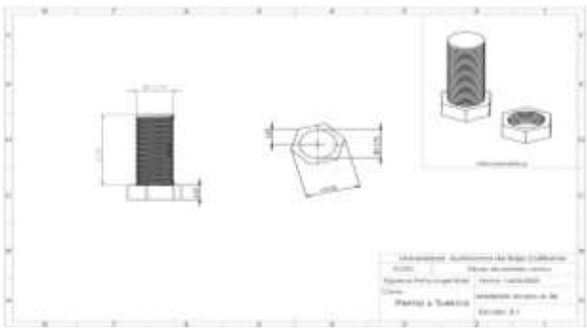

Figure 10 Bolt Drawings

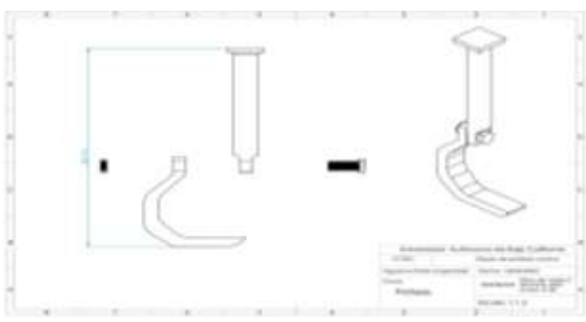

Figure 11 Assembly drawings

4. Analytical calculations

Connection pipe

For the connection tube we calculated the stress to which it would be subjected if it had a diameter of 25.40mm and it would be subjected to a load of 45 kg, which is the maximum weight over designed a can that the tube should support, therefore, we have that:

$$A = \pi\left(\frac{0.0254m}{2}\right)^2 = 0.0005m^2 \quad (1)$$

$$P = (45kg)\left(9.81\frac{m}{s^2}\right) = 441.45N \quad (2)$$

Once the cross-sectional area and weight data are obtained, the minimum stress that this part must support is obtained.

$$\sigma = \frac{441.45N}{0.0005m^2} = 882900Pa = 882.9kPa \quad (3)$$

Leg

With the geometries of the leg taking into account the base of the leg which is 0.1016m and its height of 0.127m, a right triangle is formed as shown in Figure 12.

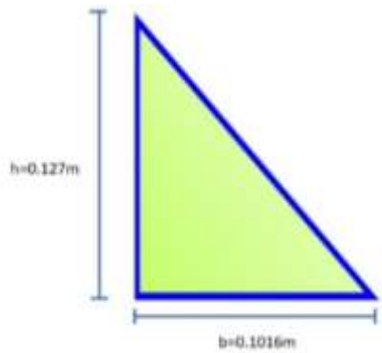

Figure 12 Construction of right triangle with measurements

With the measurements of the base and the height, we find the center of the right triangle, which is located at 1/3 of the base and 1/3 of the height. Once the center of the triangle is located, the distance from the vertices located in the X and Y components to the marked center is taken, which gives a distance of 0.09m, as shown in Figure 13.

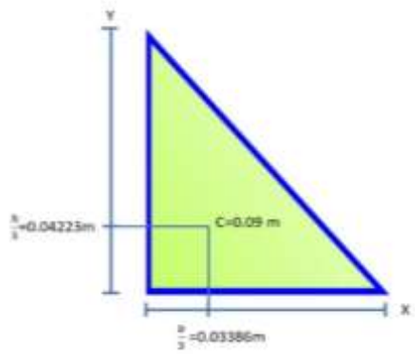

Figure 13 Distance from center to vertices

Having the distance from the center to the vertices we proceed to extract the torques acting on each component, when a load of 441.45N is applied.

$$M_y = (-441.45N)(0.09m) = -39.7305Nm \quad (4)$$

$$M_x = (441.45N)(0.09m) = 39.7305Nm \quad (5)$$

Then the moments of inertia of the cross-section with respect to the X and Y axes are calculated.

$$I_x = \frac{bh^3}{12} = \frac{(0.1016m)(0.127m)^3}{12} = 1.735x10^{-5}m^4 \quad (6)$$

$$I_y = \frac{b^3h}{12} = \frac{(0.1016m)^3(0.127m)}{12} = 1.109x10^{-5}m^4 \quad (7)$$

Once the moments of inertia have been obtained, the stresses in each axis are obtained.

$$\sigma_x = \frac{(39.7305Nm)(0.0254m)}{1.735x10^{-5}m^4} = 58.1645kPa \quad (8)$$

$$\sigma_y = \frac{(-39.7305Nm)(0.0254m)}{1.109x10^{-5}m^4} = -90.9968kPa \quad (9)$$

$$\sigma_{total} = \sigma_1 + \sigma_2 = 32.8323kPa \quad (10)$$

Bolt

The stress in each contact between the bolt and the prosthesis components was calculated.

$$\sigma = \frac{441.45N}{(0.0254m)(0.0127m)} = 1368.497kPa \quad (11)$$

5. Simulations

Once the geometries were obtained, the 3D models of the parts were made in the SolidWorks program in order to test by means of simulations the behavior of the parts that were solved by means of the finite element analysis method. Stress.

Stress concentration and displacement tests were carried out on the different components of the prosthesis, which were tested with different materials.

In the following simulations shown in Figure 14, the areas denoted by red color inside the components are the areas where a higher stress arises at the moment of applying the load.

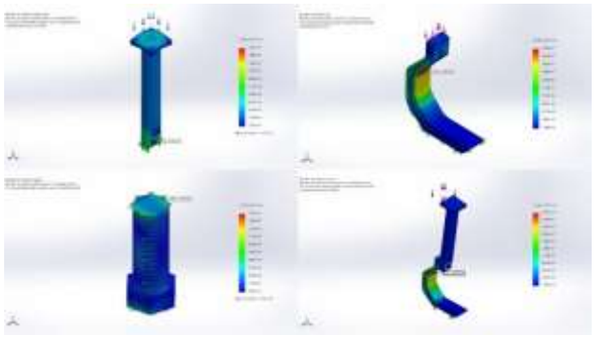

Figure 14 Stress simulations

In the following simulations, shown in Figure 15, the areas denoted by blue color are the areas where there is a higher stress concentration when a load is applied.

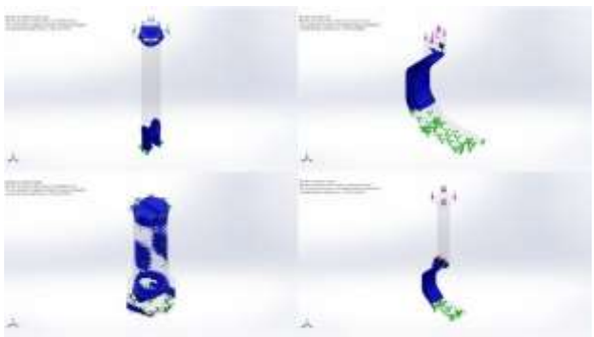

Figure 15 Stress concentration simulations

In the simulations shown in Figure 16, as in the stress simulations, the areas denoted by red color within the components are the areas where there is a greater deformation at the moment of applying the load.

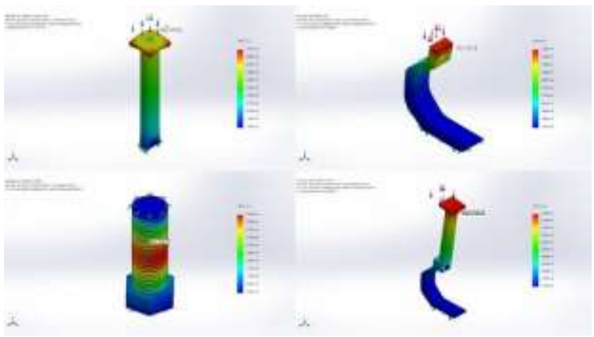

Figure 16 Displacement simulations

6. Manufacturing processes

A process analysis was carried out where the following figures show the flow diagrams that have to be followed at the moment of the fabrication of the different components of the prosthesis.

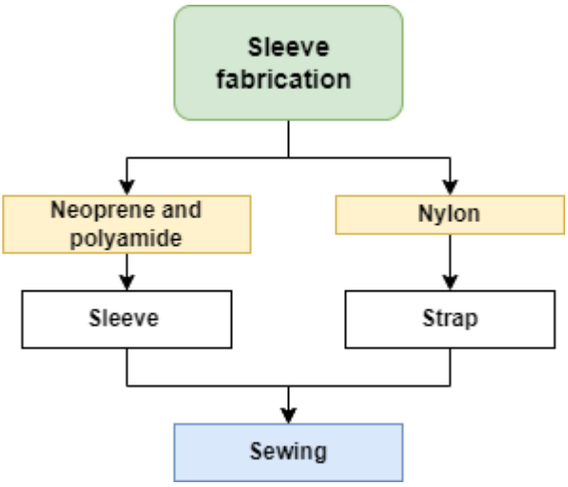

Figure 17 Flowchart of the sleeve manufacturing process

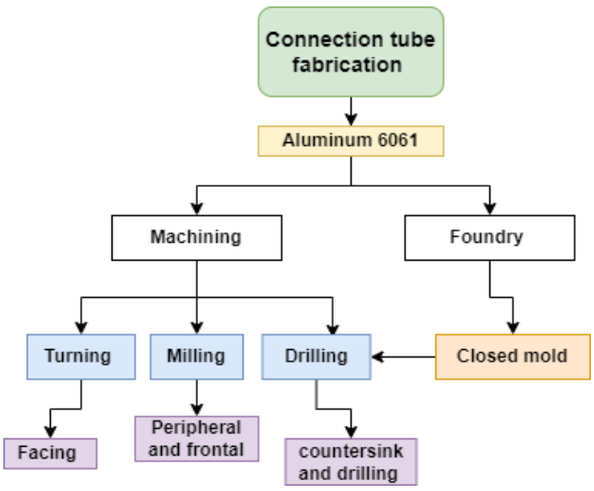

Figure 18 Flow diagram of connection tube fabrication

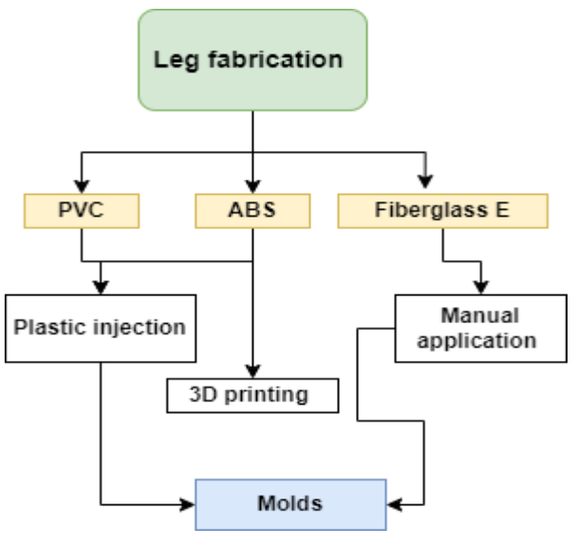

Figure 19 Leg fabrication flow diagram

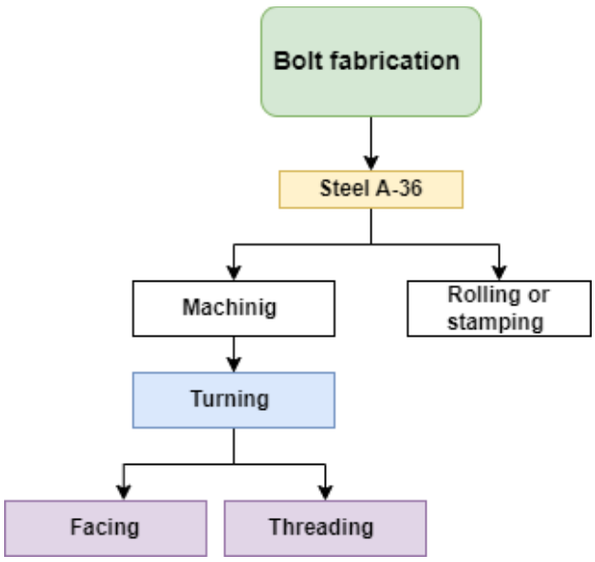

Figure 20 Bolt fabrication flowchart

7. Results

Table 1 shows the results of the components that were calculated analytically to support the minimum capacities that the parts must resist when subjected to work.

Part	Calculation	Results
Connecting tube	Area	$5x10^{-4}m^2$
	Weight	441.45N
	Effort	882.9kPa
Leg	M_y	-39.7305Nm
	M_x	39.7305Nm
	I_x	$1.735x10^{-5}$ m^4
	I_y	$1.109x10^{-5}$ m^4
	Stress 1	58.1645kPa
	Stress 2	-90.9968kPa
	Total stress	-32.8323kPa
Bolt	Stress 1	2736.995kPa
	Effort 2	2736.995kPa
	Total effort	1368.497kPa

Table 1 Concentrate of results of analytical calculations on the different components of the prosthesis

Table 2 shows the concentrate of the results obtaining values in kPa for the efforts and mm for the displacements, the part that receives a greater amount of efforts is the leg with the ABS material in the same way is the part that obtained a greater displacement with the same material, in the same way it is denoted that the areas of the parts there is in average a greater concentration of efforts is in superior area.

ISSN 2523-6849

Part	Material	Minimum stress	Maximum stress	Deformation	Area of highest stress concentration
Connecting	Aluminum 6061	75.32kPa	15350kPa	1.074x10-4mm	Upper Lower
Pipe Leg	PVC	7.218kPa	22820kPa	5.246mm	Upper
	ABS	7.837kPa	23550kPa	6.564mm	Upper
	Fiberglass E	5.153kPa	19940kPa	1.484x10-1mm	Upper
Bolt	A-36 Steel	30.92 kPa	15910kPa	5.918x10-4 mm	Central
Assembly	Various	100.299Pa	29760kPa	9.708x10-1mm	Lower

Table 2 Concentrated results of the simulations of the distribution of stresses and displacements in the canine prosthesis

8. Acknowledgement

We thank the CA of "Optimization of Mechanical Systems" for having supported the development of this article through the research project without funding, Comparative analysis of mechanical properties in 3D printed parts of the Universidad Autónoma de Baja California with code 351/3597.

9. Funding

This work has been financed by the unfunded research project, Análisis comparativo de propiedades mecánicas en piezas impresas en 3D de la Universidad Autónoma de Baja California (comparative analysis of mechanical properties in 3D printed parts of the Universidad Autónoma de Baja California, code 351/3597).

10. Conclusions

Prototype

For the prototype we have an exoprosthesis for a missing forelimb, where it must be within the range of the length of its leg from 35cm to 45cm and its weight should range between 30kg to 40kg, besides its amputation should be located from the elbow region, it will consist of four elements a sleeve, a connection tube, a bolt that acts as a pin and a leg, of which the last three of these are the components that will be subjected to significant loads, where the calculations and simulations will be carried out.

Design

For the prototype, a design process was followed in which analytical calculations and SolidWorks software were used to meet the needs or problems that arose at the time of the execution of the design stage. Thus creating the different components of the model whose combined components had a minimum stress of 100.299Pa and a maximum of 29760kPa, having a deformation of 9.708x10-1mm satisfying the geometry requirements after being simulated and tested. It should be noted that the loads were over designed in order to have a higher safety factor.

Material

For the prototype, all the different materials proposed showed to be suitable at the moment of being submitted to the loads that would be generated at the moment of being carried out the work of the prosthesis, mechanically speaking the E-glass fiber is the most suitable material at the moment of the selection of the material for the leg, although this will depend on the manufacturing process chosen.

Manufacturing process

For the prototype, the manufacturing processes will be sewing for the sleeve piece, machining for the connection tube, the bolt could also be machined but due to the easy access to these it is more profitable to get them from a tertiary supplier and for the leg the easiest process and scope is injection.

ISSN 2523-6849

Future work

As future works, the aim is to manufacture the prototype with the materials and processes proposed, as well as to look for alternatives to improve the design of the prototype.

In such a way that in this work an anterior prosthesis is proposed for a large size dog where it must be within the range of the length of its paw from 35cm to 45 cm and its weight must oscillate between 30 kg to 40 kg, besides its amputation must be located from the region of the elbow, whose combined components had a minimum effort of 100. 299Pa and a maximum of 29760kPa, having a deformation of 9.708x10-1mm, where the manufacturing processes will be, the sewing for the sleeve piece, the machining for the connection tube, the bolt is obtained by third parties and for the leg the injection.

11. References

[1] **A**lguacil Diego, A., Martínez Piedrola, M., Molina Rueda F., (2019). *Curso Online de Ortopedia y Productos de Apoyo en las Patologías más Comunes dirigido a Fisioterapeutas* [Libro electrónico]. Editorial Médica Panamericana. Recuperado 20 de agosto de 2023, de http://aula.campuspanamericana.com/_Cursos/Curso01417/Temario/Curso_Ortopeia_Productos_Apoyo/3.1.%20Curso%20Ortopedia.pdf

[2] Beer, F. P., & Johnston, E. R. (2010). *Mecánica de materiales*. McGraw-Hill Education. Recuperado 20 de agosto de 2023, de https://www.academia.edu/34453780/Mecanica_de_Materiales_5ta_Ed_Beer_Johnston_DeWolf_Mazurek_McGraw_Hill

[3] Cely B, M., Mendoza, E., & Arellana, R. (2011). Diseño y construcción de una prótesis para amputación transfemoral pediátrica con un sistema de desplazamiento vertical, validado por análisis por elementos finitos. El Hombre y la Máquina, (36), 69-76. Recuperado 20 de agosto de 2023, de https://www.redalyc.org/articulo.oa?id=47821598006

[4] Galli, K., & Pelozo, S. (2017). *Órtesis y prótesis: Monografía auditoria medica* [Libro electrónico]. Recuperado 20 de agosto de 2023, de https://www.auditoriamedicahoy.com.ar/biblioteca/Karina%20Galli%20Sabrina%20Peloso%20Ortesis%20y%20pr%C3%B3tesis.pdf

[5] Hernández, M. A., Carranza, M. A. R., Nuño, V., West, J., & Castañeda, A. P. R. (2018). Metodología para la fabricación de una prótesis transtibial a base de material compuesto de fibra de carbono y resina epóxica. Recuperado 20 de agosto de 2023, de *Materia-rio De Janeiro*, *23*(2). https://doi.org/10.1590/s1517-707620180002.0482

[6] Jaramillo, L. G. T. (2014, 30 enero). *Estudio del Arte en Protesis de Piernas*. Monografias.com. Recuperado 20 de agosto de 2023, de https://www.monografias.com/trabajos99/estudio-del-arte-protesis-piernas/estudio-del-arte-protesis-piernas

[7] Metalmecánica. (2019, 3 enero). *Nuevas estrategias para el mecanizado de piezas ortopédicas*. Recuperado 20 de agosto de 2023, de https://www.metalmecanica.com/es/noticias/nuevas-estrategias-para-el-mecanizado-de-piezas-ortopedicas

[8] Montano, L. (2022, 8 diciembre). impresion 3d | ColorPlus filamentos para impresoras 3D en México. Filamento Impresora3D. Recuperado 20 de agosto de 2023, de https://www.colorplus3d.com/impresion-3d-caso-de-exito-protesis-caninas-por-hurakan-tecnocenter/

[9] Norton, R. L. (2011). *Diseño de máquinas: un enfoque integrado*. Pearson Educación. Recuperado 20 de agosto de 2023, de https://www.udocz.com/apuntes/96659/diseno-de-maquinas-iv-edicion-robert-norton-2

[10] Prótesis. (2020, 1 febrero). American Cancer Society. Recuperado 20 de agosto de 2023, de https://www.cancer.org/es/tratamiento/tratamientos-y-efectos-secundarios/efectos-secundarios-fisicos/protesis.html

ISSN 2523-6849

[11] Roldán, L. R. (2022, 26 febrero). Guillermo Martínez, el joven que imprime brazos en 3D para personas sin recursos. The Objective. Recuperado 20 de agosto de 2023, de https://theobjective.com/sociedad/2022-02-26/protesis-brazos-3d/

[12] Zavaleta, D. V.(2020, 4 septiembre). Ortopedia para perros. Nuevas Ideas para perros especiales. Recuperado 20 de agosto de 2023, de https://www.ortocanis.com/blog/.

ISSN 2523-6849

Article **Journal of Physiotherapy and Medical Technology**
June, 2023 Vol.7 No.17 21-32

Bioinformatic evaluation and *in vivo* study of Orlistat in acute cholestatic damage

Evaluación bioinformática y estudio *in vivo* de Orlistat ante el daño agudo colestásico

ALDABA-MURUATO Liseth Rubí*†, MACÍAS-PÉREZ José Roberto, RODRIGUEZ-RODRIGUEZ Angela and ALVARADO-SÁNCHEZ Brenda

Facultad de Estudios Profesionales Zona Huasteca, Universidad Autónoma de San Luis Potosí. Romualdo del Campo No. 501, Rafael Curiel, C.P. 79060, Ciudad Valles, San Luis Potosí, México

ID 1st Author: *Liseth Rubí, Aldaba-Muruato* / **ORC ID:** 0000-0002-9641-662X, **Researcher ID Thomson:** X-3211-2018, **CVU CONAHCYT ID:** 176507

ID 1st Co-author: *José Roberto, Macías-Pérez* / **ORC ID:** 0000-0001-7925-2494, **Researcher ID Thomson:** X-2998-2018, **CVU CONAHCYT ID:** 172982

ID 2nd Co-author: *Angela, Rodríguez-Rodríguez* / **ORCID ID:** 0009-0009-6706-9954

ID 3rd Co-author: *Brenda*, Alvarado-*Sánchez* / **ORC ID:** 0000-0002-6077-2665, **CVU CONAHCYT ID:** 38716

DOI: 10.35429/JP.2023.17.7.21.32 Received March 10, 2023; Accepted June 30, 2023

Abstract

The incidence of liver diseases increases every year worldwide, making the efforts to prevent them insufficient. The present work evaluated the ability of Orlistat to prevent acute liver injury induced by ligation of the common bile duct (LCBC) in the male Wistar rat. Rats were divided into five experimental groups: untreated (NT), Sham (Sham Surgery), LCBC and LCBC+Orlistat. Serum markers of liver injury as alanine aminotransferase, alkaline phosphatase, gamma-glutamyltranspeptidase, and total and direct bilirubins were significantly increased in LCBC group relative to healthy controls. On the other hand, increases in these markers were significantly prevented in the LCBC+Orlistat group. These results were consistent with observations from livers *in situ* and with H&E-stained histological sections. In addition, the mechanism of action for Orlistat was evaluated through six protein target prediction platforms (ChEMBL, PharmMaper, SEA, Super-PRED, SwissTargetPrediction and TargetNet) where 45 possible molecules with which Orlistat could interact. Our results suggest that Orlistat has hepatoprotective activity during acute damage induced by extrahepatic cholestasis in rats.

Orlistat, Acute liver disease, Common bile duct ligation

Resumen

La incidencia de las enfermedades hepáticas continúa incrementándose cada año en todo el mundo, siendo insuficientes los esfuerzos para prevenirlas. El presente trabajo evaluó la capacidad de Orlistat para prevenir el daño hepático agudo inducido por la ligadura del conducto biliar común (LCBC) en la rata Wistar macho. Las ratas fueron divididas en cinco grupos experimentales: no tratadas (NT), Sham (Cirugía falsa), LCBC y LCBC+Orlistat. Los marcadores séricos de daño hepático alanina aminotransferasa, fosfatasa alcalina, gamma-glutamiltranspeptidasa, y las bilirrubinas totales y directas se incrementaron significativamente en el grupo LCBC en relación con los controles sanos. En el grupo LCBC+Orlistat se previnieron significativamente los aumentos en estos marcadores. Estos resultados fueron consistententes con las observaciones de los hígados in situ y con los cortes histológicos teñidos con H&E. Por otra parte, el mecanismo de acción del Orlistat fue evaluado por medio de seis plataformas de predicción de blancos proteicos (ChEMBL, PharmMaper, SEA, Super-PRED, SwissTargetPrediction y TargetNet) donde se identificaron 45 posibles moléculas con las cuales podría interactuar Orlistat. Nuestros resultados sugieren que el Orlistat posee actividad hepatoprotectora durante el daño agudo inducido por la colestasis extrahepática en rata.

Orlistat, Enfermedad hepática aguda, Ligadura de conducto biliar común

Citation: ALDABA-MURUATO Liseth Rubí, MACÍAS-PÉREZ José Roberto, RODRIGUEZ-RODRIGUEZ Angela and ALVARADO-SÁNCHEZ Brenda. Bioinformatic evaluation and *in vivo* study of Orlistat in acute cholestatic damage. Journal of Physiotherapy and Medical Technology. 2023. 7-17: 21-32

* Correspondence to the Author (e-mail: liseth.aldaba@uaslp.mx)
† Researcher contributing as first author

Introduction

The incidence and complications of liver diseases (HD) continue to increase worldwide (Moon et al., 2020). In Mexico, the HDs with the highest morbidity and mortality rates are cirrhosis and hepatocellular carcinoma (HCC), the latter being the fourth most frequent liver neoplasm in the world (Asrani et al., 2019; Llovet et al., 2021).

The aetiology of HD is multifactorial, the most common being induced by alcohol consumption and the use of drugs or toxicants that are metabolised by the liver (Mohi-Ud-Din, 2019). Obesity and metabolic syndrome favour the development of non-alcoholic steatohepatitis that can culminate in cirrhosis or HCC (Raza et al., 2021). On the other hand, the liver is also susceptible to damage by parasites such as the intestinal protozoan Entamoeba histolytica, which can migrate to the liver and necrotises it, forming an abscess known as an amoebic liver abscess (Ghelfenstein-Ferreira et al., 2020). HD can also be caused by viruses, such as viral hepatitis B and C (Sperry et al., 2022).

Furthermore, it has been reported that regardless of the aetiology, patients with chronic HD such as cirrhosis or HCC who were infected with the SARS-CoV-2 coronavirus type 2, which is the cause of the 2019 coronavirus disease (COVID-19), are vulnerable to serious liver decompensation and dysfunction events (Marjot et al., 2021).

Cholestasis is a liver disorder that occurs due to persistent obstruction of bile flow; this bile retention accumulates toxic components and increases oxidative stress, mainly damaging hepatocytes and cholangiocytes (Salas-Silva et al., 2021). Therefore, intrahepatic cholestasis occurs when alterations of the hepatic parenchyma, bile canaliculi or intrahepatic bile ducts occur, such as in patients with liver cirrhosis, virus-induced hepatitis, inflammation of the biliary tract, and inflammation of the bile ducts (Salas-Silva et al., 2021), inflammation of the bile ducts and HCC, while extrahepatic cholestasis occurs due to involvement of the extrahepatic bile ducts, common hepatic duct, or common bile duct, as in the presence of stones or tumours (Salas-Silva et al. , 2021; Hilscher et al., 2020).

In the present research work, the hepatoprotective capacity of the drug Orlistat ($C_{29}H_{53}NO_5$) was evaluated, which acts by inhibiting pancreatic and gastric lipase, thereby reducing the absorption of lipids from food, and is therefore indicated for the control of obesity (Wong & Cheng-Lai, 2000). In recent years, the scientific community has explored additional biological activities of Orlistat, for example, it was compared to the peptide Ala-Gly-Leu-Gln-Phe-Pro-Val-Gly-Arg (AGL9), a novel hepatoprotective agent, showing similar preventive effects in the non-alcoholic fatty liver disease (NAFLD) model in C57BL/6 mice (Fan et al., 2021).

Likewise, the therapeutic effect of Orlistat was evaluated by its combination with metformin, preventing systemic complications of pancreatitis, gastrointestinal, pulmonary, renal cardiac and nervous system diseases that are induced by COVID-19 in obese diabetic patients (Singh et al., 2021).

Therefore, in the present research work we aimed to determine the ability of Orlistat to reduce cholestatic liver damage that is induced by common bile duct ligation in Wistar rats.

Methodology

Experimental animals

Twenty-nine male Wistar rats (Rattus norvegicus), weighing 200-250 g, were maintained at a constant environmental temperature of 24°C, with light/dark cycles (12 h:12 h). Every day, the rat feeders and drinkers were supplied with rodent food (Labdiet 5008) and drinking water ad libitum.

Ethics

All procedures were performed in accordance with institutional guidelines for the care and use of experimental animals and with the national regulatory standard NOM-062-ZOO-1999. The present research is part of the project entitled "Evaluation of compounds with hepatoprotective activity" accepted by the Research Ethics Committee of the Facultad de Estudios Profesionales Zona Huasteca, UASLP.

ISSN 2523-6849

Experimental protocol

The hepatoprotective capacity of Orlistat was evaluated using the common bile duct ligation (CBDL) model (Van Campenhout et al., 2019; Georgiev et al., 2008). Rats were randomly divided into five groups: NT group: healthy animals without any treatment or surgical procedure (n=3); Sham group: rats were subjected to sham surgery, which consisted of exposing the bile duct without performing ligation, and were further administered prior to Sham surgery, with 1 mL daily for 10 days with 0.25% sodium carboxymethyl cellulose (CMC, Sigma-Aldrich, USA), 0.25% sodium carboxymethyl cellulose (CMC, Sigma-Aldrich, USA), 0.25% sodium carboxymethyl cellulose (CMC, Sigma-Aldrich, USA) and 0.25% sodium carboxymethyl cellulose (CMC, Sigma-Aldrich, USA). (n=4); LCBC group: rats were subjected to a surgical procedure, which allowed identification, isolation, ligation and dissection of the common bile duct, and 10 days prior to surgery, the rats were started daily with 1 mL of CMC 0.25% p.o. and continued to be administered until day 1, and 10 days before surgery, the rats were administered daily with 1 mL of CMC 0.25% p.o., and continued administration until the day of sacrifice (n=9); LCBC+Orlistat group: animals were pre-treated for 10 days with Orlistat 10 mg/kg/day, p.o., prior to LCBC and continued Orlistat administration until the day of sacrifice (n=9); and the Sham+Orlistat group (n=4). All animals were sacrificed 48 h after LCBC or sham surgeries (figure 1).

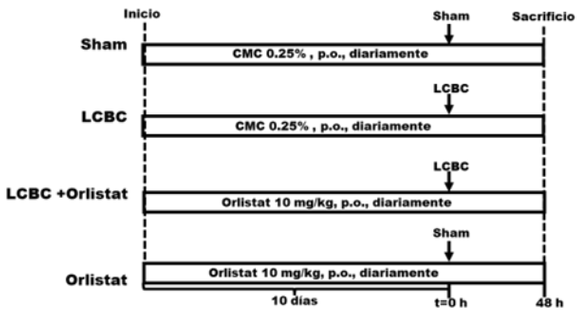

Figure 1 Experimental groups and procedures. Sham: sham surgery; p.o.: from Latin per os (via oral); LCBC: common bile duct ligation. In addition, there was a healthy group that did not undergo any of these procedures (NT group).

Surgical procedure for common bile duct ligation

The rats were anaesthetised with a mixture of Ketamine (80 mg/kg) and Xylazine (10 mg/kg) intraperitoneally (i.p.). The surgeries were performed under sterile conditions, starting with a laparotomy close to the abdominal midline of approximately 1. 5 cm in length, to expose the peritoneal cavity to observe the anatomical position of the liver and access the common bile duct, which was ligated by three knots using sterile non-absorbable surgical suture material (American braided black silk, 4-0 gauge), two knots were made close to the liver and the other at the end of the bile duct close to the duodenum, to finally cut the bile duct before the knot close to the duodenum (Van Campenhout et al., 2019; Georgiev et al., 2008).

Slaughtering the animals

To perform the sacrifices, the rats were anaesthetised with a mixture of Ketamine (80 mg/kg) and Xylazine (10 mg/kg) i.p. Blood was withdrawn by cardiac puncture, which was subsequently centrifuged at 3000 rpm and the serum obtained was used to assess markers of liver damage. The animals were checked for vital signs after blood collection and the liver tissue was dissected. Photographic images of the livers were taken in situ and then carefully dissected and washed in cold physiological saline (NaCl 0.9%) to obtain small fragments that were immersed in 4% neutral formalin and used for histological analysis.

Histological staining

Liver damage was assessed by haematoxylin & eosin (H&E) staining for morphological changes in the tissue and staining with periodic acid and Schiff's reagent (PAS) to determine the presence of carbohydrates in liver cells (Luna, 1968). For these purposes, the liver fragments obtained during animal sacrifice were fixed for 48 h with 4% neutral formalin, then washed with distilled water and subjected to a serial and gradual dehydration process of alcohol baths as follows: 70% ethanol, 85% ethanol, 96% ethanol and 100% ethanol (2 immersions at 60°C for 1 h each). Once the tissues were dehydrated, they were treated by successive baths of absolute ethanol-xylol (50:50) and xylol (2 immersions of 1 h each at 60 °C).

ISSN 2523-6849

Tissues were then embedded in liquid paraffin to create a paraffin block (Ramos-Vara 2017; Sadeghipour & Babaheidarian 2019). From the paraffin block, four micrometre thick liver sections were obtained using a hand-held rotary microtome (ECOSHEL 202A), liver sections were transferred to a flotation bath (~39 °C) and adhered to previously silanised slides (Aragón et al., 2018).

H&E staining

To perform the staining, it is necessary to deparaffinise the tissue at 60 °C for 60 min. Subsequently, the sections were rehydrated by 2 immersions of 40 s in xylene and 1 immersion in absolute ethanol-xylol (50:50), and graded series of 100 % (2 immersions), 96 % and 80 % alcohol and distilled water. Histological sections were stained with Harris haematoxylin (Sigma-Aldrich, USA) for 5 min and rinsed with tap water for 5 min. Immediately, they were immersed in acid alcohol for 10 s and rinsed for 1 min in distilled water and then passed through ammonia water for 35 s and passed through tap water for 1 min. Subsequently, slides were washed for 40 s in 80% ethanol and stained with eosin (Sigma-Aldrich, USA) for 1 min. Finally, tissues were dehydrated with 96%, 100%, alcohol-xyl alcohol (50:50) and xylol (2 dips) for 40 s each (Luna, 1968; Wick, 2019).

PAS staining

Deparaffinised tissues were immersed in 0.5% periodic acid (Sigma-Aldrich, USA) for 5 min, rinsed with distilled water for 20 s, then transferred to Schiff's reagent (Sigma-Aldrich, USA) for 15 min. They were rinsed with tap water for 5 min, then immersed in Mayer's haematoxylin (Sigma-Aldrich, USA) for 10 min and again in tap water for 5 min. Finally, the tissues were dehydrated with 40 s immersions in 96%, 100%, alcohol-xylol (50:50) and xylol (2 immersions) (Luna, 1968).

Microscopic observations

Histological stains were evaluated using an Axiostar plus brightfield microscope (HBO 50/AC, ZESS) with an adapted KOPPACE 16 MP camera (KP-1660), and were processed and analysed with S-Eye (1.6.0.11) and ImageJ (Version: 1.52) software.

Enzyme markers of liver damage in serum

Serum samples were analysed for liver damage by quantifying the enzyme activities of alanine aminotransferase (ALT), alkaline phosphatase (ALP), gamma-glutamyl transferase (GGT) (Reitman & Frankel, 1957; Bergmeyer et al., 1983; Glossmann & Neville, 1972). ALT enzyme activity was assessed in each sample in triplicate, for each test 250 µL of substrate solution (0.2 M D/L-alanine with 2 M α-ketoglutaric acid) and 50 µL of serum were added, mixed and incubated at 37°C for 60 min. Subsequently, 250 µL of the chromogenic reagent (2,4-dinitrophenylhydrazine 1 mM) was added and the sample was incubated again at the same temperature for another 15 min, finally 1.5 mL of 0.4 N NaOH was added.

The reading was done in the spectrophotometer with a wavelength of 515 nm. FA enzyme activity was determined in each sample in triplicate by adding 250 µL of 0.1 M glycine buffer and 1 mM MgCl2 at pH 10.5 and 250 µL of p-nitrophenylphosphate substrate to each sample, mixing and incubating at 37 °C for 5 min, after which time 250 µL of p-nitrophenylphosphate substrate was added to each sample. for 5 min, after which 50 µL of serum was added to incubate again at 37 °C for 30 min, finally 0.02 N NaOH was added and absorbances were measured at a wavelength of 410 nm. In each sample in triplicate, GGT enzyme activities were performed with 400 µL of 0.2 M Tris-HCl reagent, 100 µL of MgCl2, 100 µL of 0. 04 M, 100 µL of 10 mM gamma-glutamyl-p-nitroanilide were added, once the solution was prepared it was incubated for 10 min at 37°C, after this time 200 µL of the serum to be evaluated were added and incubated again for 30 min at the same temperature of 37°C, finally it was removed from incubation and 2 mL of 1.5 M acetic acid was added to stop the reaction, then they were read in a spectrophotometer with a wavelength of 410 nm.

For the three markers of liver damage, blanks were included and the respective standard curves were performed as suggested by the authors.

Total and direct bilirubin in serum

Serum total and direct bilirubin concentrations were also determined following the SPINREACT protocol (Ref: 1001044).

ISSN 2523-6849

Statistical analysis

All results obtained in this work were expressed as means ± standard error (SEM) and statistical analyses were performed using GraphPad Prism 8.00 software by one-way analysis of variance (ANOVA) followed by Tukey's test with $p<0.05$ as the significance level.

Identification of potential protein targets of Orlistat in liver

Six online platforms where protein targets of chemical compounds can be searched or predicted were consulted to analyse what kind of proteins Orlistat might interact with. The platforms used were: ChEMBL (Davies et al., 2015; Méndez et al., 2019), Pharos (Sheils et al., 2021), SEA (Keiser et al., 2007), Super-PRED (Nickel, et al., 2014), SwissTargetPrediction (Daina et al., 2019), and TargetNet (Yao et al., 2016), accessed in August 2023. On these platforms, the Orlistat molecule was entered in mol2 or SMILES formats, generated with OpenBabel software (Cheminfo.org; O'Boyle et al., 2011) where the molecule was plotted for it.

From each set of data obtained in each platform, those with the highest probability of being protein targets were chosen, according to the algorithm used in the platform (Super-PRED, SwissTargetPrediction and TargetNet), or all those returned by the platform were used. For those protein targets chosen, the GeneCards database (GeneCards; Safran et al., 2021) was searched for their homologous protein identification code. With this code, the Human Protein Atlas (Uhlén et al., 2015), a comprehensive compendium that integrates results from omics technologies to map human protein expression in cells, tissues and organs, was consulted.

Results

In situ observations of livers

The in situ livers of the NT, Sham, and Orlistat groups had a normal, dark reddish-brown appearance with shiny, smooth surfaces. The LCBC group presented a light brown liver, which is very different from the livers of the other groups when compared macroscopically. The LCBC+Orlistat group showed an appearance mostly similar to the healthy groups than the LCBC group (figure 2).

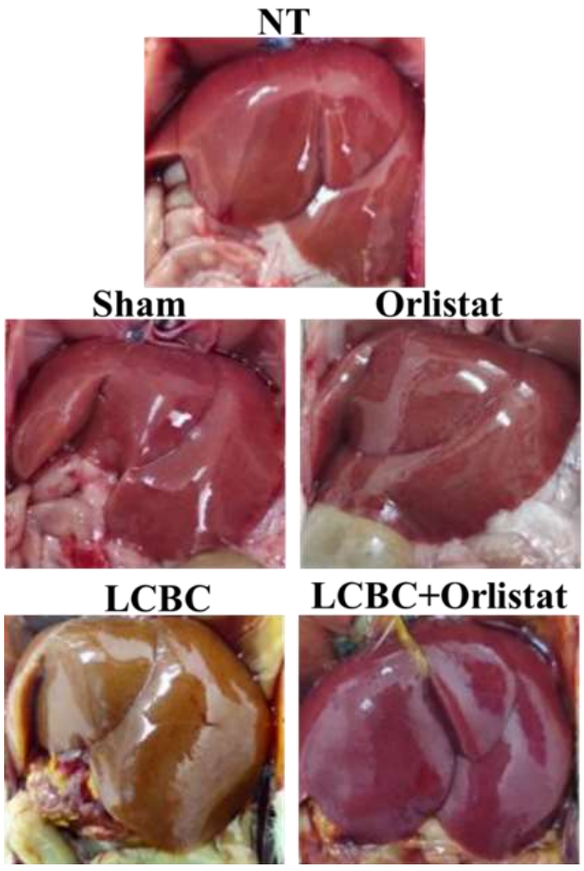

Figure 2 Representative images of livers observed in situ from the different experimental groups

Histological staining

The microscopic observations were consistent with the results in Figure 3, the healthy groups were observed with a well-structured liver parenchyma, while the animals in the LCBC group showed necrosis, inflammation and ductal proliferation, and in the rats of the LCBC+Orlistat group a decrease in liver damage was observed compared to the LCBC group.

ISSN 2523-6849

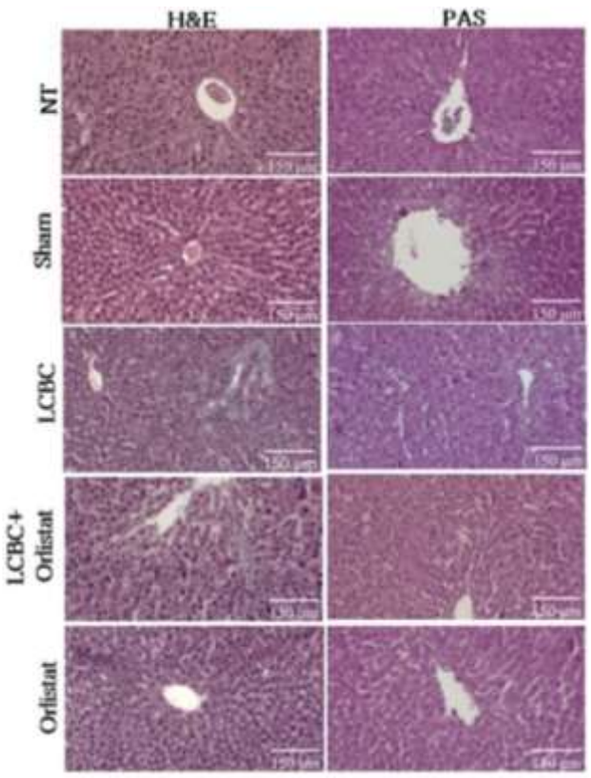

Figure 3 Representative images of histological sections stained with H&E or PAS.

Serum markers of liver damage

ALT, FA and GGT enzyme activities were significantly increased in the LCBC group animals compared to the healthy groups. On the other hand, the LCBC+Orlistat group showed a partial but significant prevention when compared to the healthy and LCBC groups. ALT, FA and GGT enzyme activities were not significantly different between the healthy groups (Figure 4).

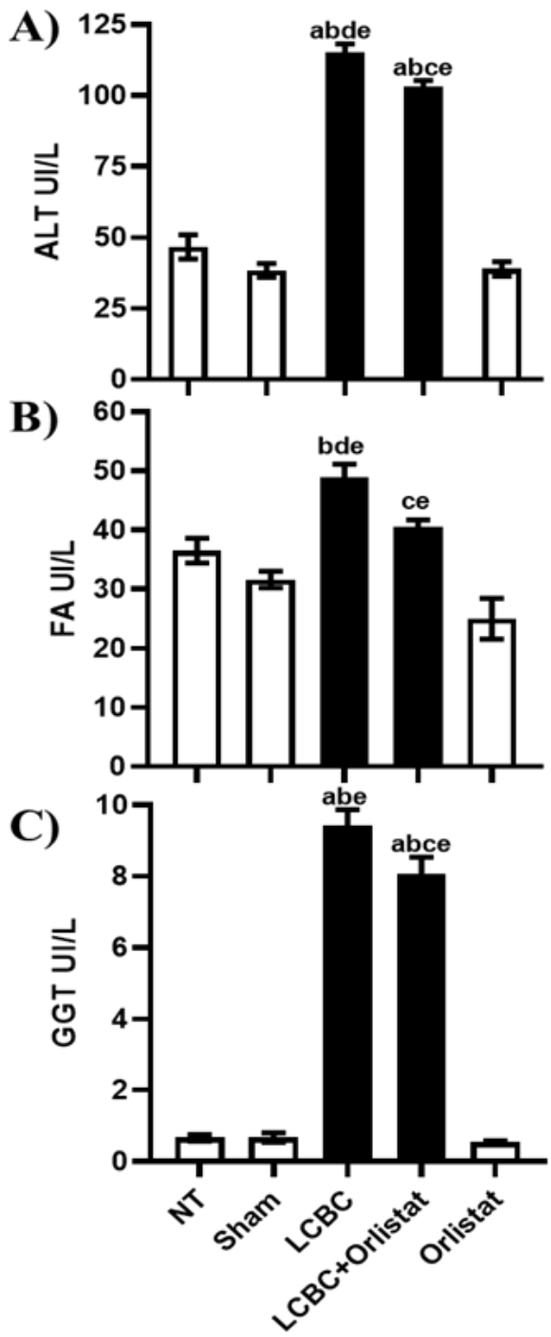

Figure 4 Measurement of liver damage markers in plasma A) ALT, B) FA, C) GGT. Significance $p<0.05$. a: significantly different from NT group; b: significantly different from Sham group; c: significantly different from LCBC group; d: significantly different from LCBC+Orlistat group; e: significantly different from Orlistat group.

Total and direct bilirubin

Total and direct bilirubin increased significantly in the LCBC group, while the LCBC+Orlistat group showed a trend that was not statistically different from the LCBC group. No significant differences were shown between the healthy control groups (Figure 5).

ISSN 2523-6849

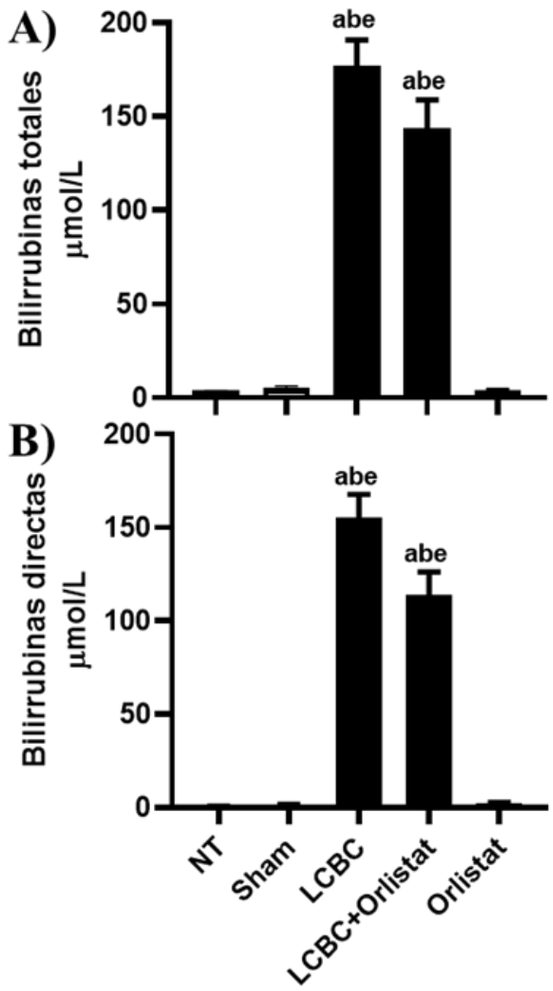

Figure 5 Determination of bilirubin**.** A) Total bilirubin, B) Direct bilirubin. Significance p<0.05. a: significantly different with respect to the NT group; b: different with respect to the Sham group; e: different with respect to the Orlistat group

Identification of potential protein targets of Orlistat in liver

Table 1 shows the 45 potential protein targets of Orlistat that were identified in the different platforms, which were selected based on the information stored in the Human Protein Atlas, either because they are expressed in the liver, enriched in hepatocytes, hepatic stellate cells or Kupffer cells (liver-specific macrophages), as well as for their involvement in liver-specific functions, angiogenesis processes, their relationship with nuclear factor kappa-B (NF□B) or with known prognostic markers of liver cancer. The latter represent 46.6% of Orlistat's potential protein targets. Shown here are the target name, its universal protein identifier code, the selection information from the Human Protein Atlas and the Platform on which it was identified as a potential target.

Tabla 1. Posibles blancos proteicos de Orlistat en hígado.

Nombre de la proteína blanco	ID de la proteína	Ubicación y/o función del blanco	Plataforma de búsqueda de blanco
Bomba de exportación de sales biliares (Bile salt export pump)	ABCB11	Tejido enriquecido: Hígado	Ch
Proteína 1 asociada a la resistencia a múltiples fármacos (Multidrug resistance-associated protein 1)	ABCC1	Marcador pronóstico en cáncer de hígado (no favorable)	SP
Transportador canalicular multiespecífico de aniones orgánicos 1 (Canalicular multispecific organic anion transporter 1)	ABCC2	Tejido, incrementado: Hígado	Ch
Transportador canalicular multiespecífico de aniones orgánicos 2 (Canalicular multispecific organic anion transporter 2)	ABCC3	Tejido, incrementado: Hígado	Ch
Monoacilglicerol lipasa ABHD12 (Monoacylglycerol lipase ABHD12)	ABHD12	Marcador pronóstico en cáncer de hígado (no favorable)	SP, Ch, S, Ph
Monoacilglicerol lipasa ABHD6 (Monoacylglycerol lipase ABHD6)	ABHD6	Tejido, incrementado: Hígado	ST, SP, Ch, S, Ph
ADN-(sitio apurínico o apirimidínico) liasa (DNA-(apurinic or apyrimidinic site) lyase)	APEX1	Marcador pronóstico en cáncer de hígado (no favorable)	SP
Ataxina-2 (Ataxin-2)	ATXN2	Marcador pronóstico en cáncer de hígado (no favorable)	Ch
Homólogo 1 de la proteína Chromobox (Chromobox protein homolog 1)	CBX1	Marcador pronóstico en cáncer de hígado (no favorable)	Ch
Fosfatasa 2 del Inductor de fase M (M-phase inducer phosphatase 2)	CDC25B	Marcador pronóstico en cáncer de hígado (no favorable)	TN
Catepsina B (Cathepsin B)	CTSB	Tipo celular, incrementado: Células de Kupffer	TN
Catepsina L (Cathepsin L)	CTSL	Tipo celular, incrementado: Células estrelladas hepáticas	SP, TN
Citocromo P450 2A6 (Cytochrome P450 2A6)	CYP2A6	Tejido enriquecido: Hígado	SP
Citocromo P450 2C9 (Cytochrome P450 2C9)	CYP2C9	Tejido enriquecido: Hígado	Ch
Citocromo P450 2D6 (Cytochrome P450 2D6)	CYP2D6	Tejido enriquecido: Hígado	Ch
Citocromo P450 3A4 (Cytochrome P450 3A4)	CYP3A4	Tejido enriquecido: Hígado	Ch, SP
Sintasa de ácidos grasos (Fatty acid synthase)	FASN	Angiogénesis (no específica)	Ch, S, Ph
Glutamato carboxipeptidasa 2 (Glutamate carboxypeptidase 2)	FOLH1	Marcador pronóstico en cáncer de hígado (favorable)	TN
Receptor 1 de formil péptido (Formyl peptide receptor 1)	FPR1	Tipo celular enriquecido: Células de Kupffer	SP
Receptor de lipoxina A4 (Lipoxin A4 receptor)	FPR2	Tipo celular, incrementado: Células de Kupffer	SP
Geranilgeranil pirofosfato sintetasa (Geranylgeranyl pyrophosphate synthetase)	GGPS1	Marcador pronóstico en cáncer de hígado (no favorable)	SP
Lipasa hepática (Hepatic lipase)	LIPC	Tejido enriquecido: Hígado	SP, Ch, Ph
Lipasa endotelial (Endothelial lipase)	LIPG	Tipo celular, incrementado: Hepatocitos	SP, Ch, Ph
Acil-proteína tioesterasa 2 (Acyl-protein thioesterase 2)	LYPLA2	Marcador pronóstico en cáncer de hígado (no favorable)	S
Menin (Menin)	MEN1	Marcador pronóstico en cáncer de hígado (no favorable)	Ch*
Monoglicérido lipasa (Monoglyceride lipase)	MGLL	Angiogénesis (no específica)	Ch
Subunidad p105 del factor nuclear NF-kappa-B (Nuclear factor NF-kappa-B p105 subunit)	NFKB1	Subunidad de NFκB	SP
Proteína 1 similar a C1 de Niemann-Pick (Nuclear factor NF-kappa-B p105 subunit)	NPC1L1	Tejido enriquecido: Hígado	Ch
Receptor de pregnano X (Pregnane X receptor)	NR1I2	Tejido enriquecido: Hígado	Ch, SP
PI3-cinasa p110-subunidad delta (PI3-kinase p110-delta subunit)	PIK3CD	Tipo celular, incrementado: Células de Kupffer	SP
PI3-cinasa p110-alfa/p85-alfa (PI3-kinase p110-alpha/p85-alpha)	PIK3R1	Marcador pronóstico en cáncer de hígado (favorable)	SP
Proteína cinasa C delta (Protein kinase C delta)	PRKCD	Marcador pronóstico en cáncer de hígado (no favorable)	SP
Subunidad Macropaín del Proteasoma (Proteasome Macropain subunit)	PSMB2	Marcador pronóstico en cáncer de hígado (no favorable)	Ch
Subunidad Macropaín del Proteasoma, MB1 (Proteasome Macropain subunit MB1)	PSMB5	Marcador pronóstico en cáncer de hígado (no favorable)	Ch
Factor de intercambio de nucleótidos de guanina 3 de Rap (Rap guanine nucleotide exchange factor 3)	RAPGEF3	Angiogénesis (no específica)	Ch
Subunidad beta del factor de unión al núcleo (Core-binding factor subunit beta)	CBFB	Marcador pronóstico en cáncer de hígado (no favorable)	Ch*
Subunidad alfa de la proteína del canal de sodio tipo IV (Sodium channel protein type IV alpha subunit)	SCN4A	Angiogénesis (adipocitos y células endoteliales)	SP
Miembro 1 de la familia 40 de transportadores de solutos (Solute carrier family 40 member 1)	SLC40A1	Tipo celular, incrementado: Células de Kupffer	SP
Miembro 1B1 de la familia de transportadores de aniones orgánicos y transportador de solutos (Solute carrier organic anion transporter family member 1B1)	SLCO1B1	Tejido enriquecido: Hígado	Ch
Miembro 1B3 de la familia de transportadores de aniones orgánicos y transportador de solutos (Solute carrier organic anion transporter family member 1B3)	SLCO1B3	Tejido enriquecido: Hígado	Ch
Tirosil-ADN fosfodiesterasa 1 (Tyrosyl-DNA phosphodiesterase 1)	TDP1	Marcador pronóstico en cáncer de hígado (no favorable)	Ch, SP
Receptor tipo Toll 4 (Toll-like receptor 4)	TLR4	Tipo celular, incrementado: Células de Kupffer, Células estrelladas hepáticas	SP
Proteasa transmembrana serina 6 (Transmembrane protease serine 6)	TMPRSS6	Tejido enriquecido: Hígado	SP
Factor intermediario de transcripción 1-alfa (Transcription intermediary factor 1-alpha)	TRIM24	Marcador pronóstico en cáncer de hígado (no favorable)	SP
Ubiquitina carboxilo-terminal hidrolasa 1 (Ubiquitin carboxyl-terminal hydrolase 1)	USP1	Marcador pronóstico en cáncer de hígado (no favorable)	Ch

El símbolo * indica que el blanco es parte de un complejo proteico, no una proteína individual. Ch-ChEMBL, PM-PharmMapper, Ph-Pharos, S-SEA, SP-Super-PRED, ST-SwissTargetPrediction, TN-TargetNet.

Discussion

Of the liver pathologies, cholestatic diseases are the least studied, so their mechanisms of damage remain poorly understood (Salas-Silva et al., 2021). Cholangiopathies are associated with direct damage to the biliary epithelium and inflammatory processes, such as primary sclerosing cholangitis, primary biliary cholangitis, biliary atresia, cystic fibrosis, drug-induced cholangiopathies, cholangiocarcinoma, among others (Salas-Silva et al., 2019; Guicciardi et al., 2013). In the present study, the hepatoprotective effect of Orlistat on acute liver damage induced by extrahepatic bile duct obstruction was evaluated in Wistar rats. The liver is composed of different cell types, such as hepatocytes, Kupffer cells, hepatic stellate cells, NK (natural killer) cells, hepatic sinusoidal endothelial cells and cholangiocytes, of which hepatocytes and cholangiocytes are the most affected during cholestasis damage (Salas-Silva et al., 2021; Salas-Silva et al., 2019; Guicciardi et al., 2013).

ISSN 2523-6849

In the present work, rats were subjected for a period of 48 h to extrahepatic obstruction of bile flow induced by ligation of the common bile duct, In the LCBC rats, a significant increase in hepatocyte necrosis was observed based on the evaluation of serum ALT enzyme activity and hepatic histological sections stained with H&E and PAS. In addition to evidence of hepatocellular necrosis, increases in cholestasis markers FA and GGT were observed, as well as ductal proliferation, which is another indicator of cholangiocyte damage. Bile ductal proliferation involves massive necrosis of hepatocytes (Guicciardi et al., 2013).

On the other hand, pretreatment with Orlistat in the LCBC+Orlistat group was able to partially prevent liver damage due to cholestasis, observing in situ livers with a macroscopic morphology with fewer alterations compared to the livers of the LCBC group, likewise, histological staining with HE and PAS, Also, histological staining with HE and PAS showed liver parenchymal architecture with less presence of necrosis and bile duct proliferation, and consistent with these observations the liver damage markers ALT, FA and GGT were partially but significantly prevented from increasing in relation to the healthy and LCBC groups. Orlistat is a drug that is prescribed for weight loss, and although in 2010 the FDA (Food and drug administration) announced the existence of clinically attributed liver damage to its use, the hepatotoxicity of Orlistat is considered controversial and far from proven (In LiverTox, 2020).

In the present study, in the group of rats treated only with Orlistat at a dose of 10 mg/kg, p.o., daily (Orlistat group), no enzymatic markers of liver damage were altered, nor were differences in liver architecture observed when compared to the healthy NT and Sham groups. On the other hand, an article was recently published on the effect of Orlistat in the treatment of patients with NAFLD, a disease characterised by excessive lipid accumulation, inflammation and fibrosis, which can progress to cirrhosis or HCC; demonstrating that Orlistat can serve as a treatment in NAFLD (Ye et al., 2019). In addition, Orlistat possesses protective and therapeutic activity in rats with fatty liver disease associated with metabolic dysfunction (MAFLD previously called NAFLD) through activation of nuclear factor erythroid-derived factor 2-like factor 2 (Nrf2), which reduces oxidative stress (Zakaria et al., 2021).

The transcriptional factor Nrf2 is a regulator of the antioxidant response, through antioxidant response element-mediated gene expression, is expressed in many organs, but primarily in liver, enabling liver cells to combat oxidative stress during the development of liver diseases (Tang et al., 2014). However, given the history of its potential hepatotoxicity, further research is needed into its potential uses as a hepatoprotectant and the improvement of dose concentration or combination with other drugs.

Moreover, the present study being one of the first to evaluate the direct effect of Orlistat in a model of in vivo cholestasis liver damage, it was decided to consult online platforms to predict possible molecular targets of Orlistat, which are mainly expressed in the liver, and which could be targets for further research. Of the 45 protein targets identified, the protein coded ABCB11 is a bile salt export pump (BSEP), and mutations in it are associated with cholestatic liver disease (Kubitz et al., 2012), and given the possible interaction with Orlistat, further studies are needed to determine its mechanism of action.

In addition, interest arises in evaluating the bioactive effect of predicted interactions of Orlistat with prognostic markers of liver cancer such as ABCC1, ABHD12, APEX1, ATXN2, CBX1, CDC25B, GGPS1, LYPLA2, MEN1, PRKCD, PSMB2, PSMB5, CBFB, TDP1, TRIM24 and USP1 and identifying possible interaction with (favourable) liver cancer prognostic markers such as CYP2A6, CYP2C9, FOLH1, PIK3R1 and TMPRSS6. Another molecule we identified was NFKB1, which is a suppressor of inflammation and cancer (Cartwright et al., 2016). Orlistat has been shown to reduce colon cancer promotion in mice by suppressing inflammation by inhibiting NFKB activity (Jin et al., 2021).

Therefore, the hepatoprotective results of Orlistat obtained in this work could be mediated by this transcriptional factor, which makes it a molecule that should be explored to try to elucidate the mechanism of action, and a structure activity relationship study (QSAR) would allow the hepatoprotective effect to be optimised.

ISSN 2523-6849

Conclusion

Our results suggest for the first time that Orlistat can reduce cholestatic liver damage induced by acute common bile duct obstruction in Wistar rats. Bioinformatic analysis yields different possible therapeutic targets that open the possibility of diverse mechanisms of action, which can be explored in future projects and the opportunity arises to study the structure-activity relationship with Orlistat analogues and derivatives, in search of optimising its therapeutic effect.

Acknowledgements

The authors are grateful for the technical support of LQC Teresa de Jesús Barrios Hurtado, and also thank CONACYT for the support granted with project 320331, in the framework of the "Basic and/or Frontier Science Modality: Paradigms and Controversies of Science 2022" call for proposals.

Funding

The authors thank CONACYT for funding No. 320331 "Basic and/or Frontier Science Modality: Paradigms and Controversies of Science 2022".

References

Aragón, P., Noguera, P., Bañuls, M. J., Puchades, R., Maquieira, Á., & González-Martínez, M. Á. (2018). Modulating receptor-ligand binding in biorecognition by setting surface wettability. Analytical and bioanalytical chemistry, 410(23), 5723–5730. https://doi.org/10.1007/s00216-018-1247-8

Asrani, S. K., Devarbhavi, H., Eaton, J., & Kamath, P. S. (2019). Burden of liver diseases in the world. Journal of hepatology, 70(1), 151–171. https://doi.org/10.1016/j.jhep.2018.09.014
Bergmeyer, H. U., Grabl, M. & Walter, H. E. (1983). Enzymes, in Methods of Enzymatic Analysis, Edited by J. Bergmeyer, Editor. p. 269 –270.

Cartwright, T., Perkins, N. D., & L Wilson, C. (2016). NFKB1: a suppressor of inflammation, ageing and cancer. The FEBS journal, 283(10), 1812–1822. https://doi.org/10.1111/febs.13627

Cheminfo.org. (2022). OPENBABEL - Chemical file format converter. Cheminfo.org. http://www.cheminfo.org/Chemistry/Cheminformatics/FormatConverter/index.html#

Daina, A., Michielin, O., & Zoete, V. SwissTargetPrediction: updated data and new features for efficient prediction of protein targets of small molecules, 2019, Nucleic Acids Research, 47(W1), W357–W3664. https://doi.org/10.1093/nar/gkz382

Davies, M., Nowotka, M., Papadatos, G., Dedman, N., Gaulton, A., Atkinson, F., Bellis, L., & Overington, J. P. (2015). ChEMBL web services: streamlining access to drug discovery data and utilities. Nucleic acids research, 43(W1), W612–W620. https://doi.org/10.1093/nar/gkv352

Fan, M., Choi, Y. J., Tang, Y., Kim, J. H., Kim, B. G., Lee, B., Bae, S. M., & Kim, E. K. (2021). AGL9: A Novel Hepatoprotective Peptide from the Larvae of Edible Insects Alleviates Obesity-Induced Hepatic Inflammation by Regulating AMPK/Nrf2 Signaling. Foods (Basel, Switzerland), 10(9), 1973. https://doi.org/10.3390/foods10091973

GeneCards - The Human Gene Database. GeneCardsSuite. https://www.genecards.org/

Georgiev, P., Jochum, W., Heinrich, S., Jang, J. H., Nocito, A., Dahm, F., & Clavien, P. A. (2008). Characterization of time-related changes after experimental bile duct ligation. The British journal of surgery, 95(5), 646–656. https://doi.org/10.1002/bjs.6050

Ghelfenstein-Ferreira, T., Gits-Muselli, M., Dellière, S., Denis, B., Guigue, N., Hamane, S., Alanio, A., & Bretagne, S. (2020). Entamoeba histolytica DNA Detection in Serum from Patients with Suspected Amoebic Liver Abscess. Journal of clinical microbiology, 58(10), e01153-20. https://doi.org/10.1128/JCM.01153-20.

Glossmann, H., & Neville, D. M. (1972). gamma-Glutamyltransferase in kidney brush border membranes. FEBS letters, 19(4), 340–344. https://doi.org/10.1016/0014-5793(72)80075-9

ISSN 2523-6849

Guicciardi, M. E., Malhi, H., Mott, J. L., & Gores, G. J. (2013). Apoptosis and necrosis in the liver. Comprehensive Physiology, 3(2), 977–1010. https://doi.org/10.1002/cphy.c120020

Hilscher, M. B., Kamath, P. S., & Eaton, J. E. (2020). Cholestatic Liver Diseases: A Primer for Generalists and Subspecialists. Mayo Clinic proceedings, 95(10), 2263–2279. https://doi.org/10.1016/j.mayocp.2020.01.015

Jin, B. R., Kim, H. J., Sim, S. A., Lee, M., & An, H. J. (2021). Anti-Obesity Drug Orlistat Alleviates Western-Diet-Driven Colitis-Associated Colon Cancer via Inhibition of STAT3 and NF-κB-Mediated Signaling. Cells, 10(8), 2060. https://doi.org/10.3390/cells10082060

Keiser, M. J., Roth, B. L., Armbruster, B. N., Ernsberger, P., Irwin, J. J., & Shoichet, B. K. Relating protein pharmacology by ligand chemistry, 2007, Nature Biotechnology, 25(2), 197–206. https://doi.org/10.1038/nbt1284

Kubitz, R., Dröge, C., Stindt, J., Weissenberger, K., & Häussinger, D. (2012). The bile salt export pump (BSEP) in health and disease. Clinics and research in hepatology and gastroenterology, 36(6), 536–553. https://doi.org/10.1016/j.clinre.2012.06.006

LiverTox: Clinical and Research Information on Drug-Induced Liver Injury [Internet]. Bethesda (MD): National Institute of Diabetes and Digestive and Kidney Diseases; 2012-. Orlistat. [Updated 2020 Jun 4]. Available from: https://www.ncbi.nlm.nih.gov/books/NBK548898/

Llovet, J. M., Kelley. R.K., Villanueva, A., Singal, A. G., Roayaie, S., Lencioni, R., Koike, K., Zucman-Rossi, J., & Finn, R. S. (2021). Hepatocellular carcinoma, Nature reviews Disease Primers, 7, 6. https://doi.org/10.1038/s41572-020-00240-3

Luna, L. G., Manual of histologic staining methods of the Arme Forces Institute of Pathology. 1968. New York: McGraw-Hill. 3rd ed.

Marjot, T., Webb, G. J., Barritt, A. S., 4th, Moon, A. M., Stamataki, Z., Wong, V. W., & Barnes, E. (2021). COVID-19 and liver disease: mechanistic and clinical perspectives. Nature reviews. Gastroenterology & hepatology, 18(5), 348–364. https://doi.org/10.1038/s41575-021-00426-4

Méndez, D., Gaulton, A., Bento, A. P., Chambers, J., De Veij, M., Félix, E., Magariños, M. P., Mosquera, J. F., Mutowo, P., Nowotka, M., Gordillo-Marañón, M., Hunter, F., Junco, L., Mugumbate, G., Rodríguez-López, M., Atkinson, F., Bosc, N., Radoux, C. J., Segura-Cabrera, A., Hersey, A., Leach, A. R. ChEMBL: Towards direct deposition of bioassay data, 2019, Nucleic Acids Research, 47(D1), D930–D940. https://doi.org/10.1093/nar/gky1075

Mohi-Ud-Din, R., Mir, R. H., Sawhney, G., Dar, M. A., & Bhat, Z. A. (2019). Possible Pathways of Hepatotoxicity Caused by Chemical Agents. Current drug metabolism, 20(11), 867–879. https://doi.org/10.2174/1389200220666191105121653

Moon, A. M., Singal, A. G., & Tapper, E. B. (2020). Contemporary Epidemiology of Chronic Liver Disease and Cirrhosis. Clinical gastroenterology and hepatology: the official clinical practice journal of the American Gastroenterological Association, 18(12), 2650–2666. https://doi.org/10.1016/j.cgh.2019.07.060 Nickel, J., Gohlke, B. O., Erehman, J., Banerjee, P., Rong, W. W., Goede, A., Dunkel, M., & Preissner, R. SuperPred: Update on drug classification and target prediction, 2014, Nucleic Acids Research, 42(W1), 26–31. https://doi.org/10.1093/nar/gku477

O'Boyle, N. M., Banck, M., James, C. A., Morley, C., Vandermeersch, T., & Hutchison, G. R. Open Babel: An Open chemical toolbox, 2011, Journal of Cheminformatics 3(10), 33. https://doi.org/10.1186/1758-2946-3-33

Ramos-Vara J. A. (2017). Principles and Methods of Immunohistochemistry. Methods in molecular biology (Clifton, N.J.), 1641, 115–128. https://doi.org/10.1007/978-1-4939-7172-5_5

ISSN 2523-6849

Raza, S., Rajak, S., Upadhyay, A., Tewari, A., & Anthony Sinha, R. (2021). Current treatment paradigms and emerging therapies for NAFLD/NASH. Frontiers in bioscience (Landmark edition), 26(2), 206–237. https://doi.org/10.2741/4892

Reitman, S,. & Frankel, S. (1957). A colorimetric method for the determination of serum glutamic oxalacetic and glutamic pyruvic transaminases. American journal of clinical pathology, 28(1), 56–63. https://doi.org/10.1093/ajcp/28.1.56

Sadeghipour, A., & Babaheidarian, P. (2019). Making Formalin-Fixed, Paraffin Embedded Blocks. Methods in molecular biology (Clifton, N.J.), 1897, 253–268. https://doi.org/10.1007/978-1-4939-8935-5_22

Safran, M., Rosen, N., Twik, M., BarShir, R., Stein, T. I., Dahary, D., Fishilevich, S., & Lancet, D. (2021). The GeneCards Suite. En I. Abugessaisa & T. Kasukawa (Eds.), Practical Guide to Life Science Databases, Springer Singapore, 1a ed., pp. 27–56. https://doi.org/10.1007/978-981-16-5812-9_2

Salas-Silva S, Simoni-Nieves A, López-Ramírez J, Bucio L, Gómez-Quiroz LE, Gutierrez-Ruiz MC, et al. Cholangiocyte death in ductopenic cholestatic cholangiopathies: Mechanistic basis and emerging therapeutic strategies, 2019, Life Sci, 218:324–39.

Salas-Silva, S., Simoni-Nieves, A., Chávez-Rodríguez, L., Gutiérrez-Ruiz, M. C., Bucio, L., & Quiroz, L. E. G. (2021). Mechanism of cholangiocellular damage and repair during cholestasis. Annals of hepatology, 26, 100530. https://doi.org/10.1016/j.aohep.2021.100530

Sheils, T. K., Mathias, S. L., Kelleher, K. J., Siramshetty, V. B., Nguyen, D. T., Bologa, C. G., Jensen, L. J., Vidović, D., Koleti, A., Schürer, S. C., Waller, A., Yang, J. J., Holmes, J., Bocci, G., Southall, N., Dharkar, P., Mathé, E., Simeonov, A., & Oprea, T. I. TCRD and Pharos 2021: Mining the human proteome for disease biology, 2021. Nucleic Acids Research, 49(D1), D1334–D1346. https://doi.org/10.1093/nar/gkaa993

Singh, Y., Gupta, G., Anand, K., Kumar Jha, N., Thangavelu, L., Kumar Chellappan, D., & Dua, K. (2021). Molecular exploration of combinational therapy of orlistat with metformin prevents the COVID-19 consequences in obese diabetic patients. European review for medical and pharmacological sciences, 25(2), 580–582. https://doi.org/10.26355/eurrev_202101_24614

Sperry, A. B., Bennett, A., & Wen, J. (2022). Hepatitis B and C in Children. Clinics in liver disease, 26(3), 403–420. https://doi.org/10.1016/j.cld.2022.03.005

Tang, W., Jiang, Y. F., Ponnusamy, M., & Diallo, M. (2014). Role of Nrf2 in chronic liver disease. World journal of gastroenterology, 20(36), 13079–13087. https://doi.org/10.3748/wjg.v20.i36.13079

Uhlén, M., Fagerberg, L., Hallström, B. M., Lindskog, C., Oksvold, P., Mardinoglu, A., Sivertsson, Å., Kampf, C., Sjöstedt, E., Asplund, A., Olsson, I., Edlund, K., Lundberg, E., Navani, S., Szigyarto, C. A.-K., Odeberg, J., Djureinovic, D., Takanen, J. O., Hober, S., … Pontén, F. Tissue-based map of the human proteome. Science, 2015, Proteomics. New York, N.Y., 347(6220), 1260419. https://doi.org/10.1126/science.1260419

Van Campenhout, S., Van Vlierberghe, H., & Devisscher, L. (2019). Common Bile Duct Ligation as Model for Secondary Biliary Cirrhosis. Methods in molecular biology (Clifton, N.J.), 1981, 237–247. https://doi.org/10.1007/978-1-4939-9420-5_15

Wick M. R. (2019). The hematoxylin and eosin stain in anatomic pathology-An often-neglected focus of quality assurance in the laboratory. Seminars in diagnostic pathology, 36(5), 303–311. https://doi.org/10.1053/j.semdp.2019.06.003

Wong, N. N., & Cheng-Lai, A. (2000). Orlistat. Heart disease (Hagerstown, Md.), 2(2), 174–181.

Yao, Z. J., Dong, J., Che, Y. J., Zhu, M. F., Wen, M., Wang, N. N., Wang, S., Lu, A. P., & Cao, D. S. TargetNet: a web service for predicting potential drug–target interaction profiling via multi-target SAR models, 2016, Journal of Computer-Aided Molecular Design, 30(5), 413–424. https://doi.org/10.1007/s10822-016-9915-2

ISSN 2523-6849

Ye, J., Wu, Y., Li, F., Wu, T., Shao, C., Lin, Y., Wang, W., Feng, S., & Zhong, B. Effect of orlistat on liver fat content in patients with nonalcoholic fatty liver disease with obesity: assessment using magnetic resonance imaging-derived proton density fat fraction, 2019, Therapeutic advances in gastroenterology, 12, 1756284819879047. https://doi.org/10.1177/1756284819879047

Zakaria, Z., Othman, Z. A., Bagi Suleiman, J., Jalil, N. A. C., Ghazali, W. S. W., & Mohamed, M. (2021). Protective and Therapeutic Effects of Orlistat on Metabolic Syndrome and Oxidative Stress in High-Fat Diet-Induced Metabolic Dysfunction-Associated Fatty Liver Disease (MAFLD) in Rats: Role on Nrf2 Activation. Veterinary sciences, 8(11), 274. https://doi.org/10.3390/vetsci8110274

ISSN 2523-6849

[Title in Times New Roman and Bold No. 14 in English and Spanish]

Surname (IN UPPERCASE), Name 1st Author†*, Surname (IN UPPERCASE), Name 1st Coauthor, Surname (IN UPPERCASE), Name 2nd Coauthor and Surname (IN UPPERCASE), Name 3rd Coauthor

Institutional Affiliation of Author including Dependency (No.10 Times New Roman and Italic)

International Identification of Science - Technology and Innovation

ID 1st Author: (ORC ID - Researcher ID Thomson, arXiv Author ID - PubMed Author ID - Open ID) and CVU 1st author: (Scholar-PNPC or SNI-CONAHCYT) (No.10 Times New Roman)

ID 1st Coauthor: (ORC ID - Researcher ID Thomson, arXiv Author ID - PubMed Author ID - Open ID) and CVU 1st coauthor: (Scholar or SNI) (No.10 Times New Roman)

ID 2nd Coauthor: (ORC ID - Researcher ID Thomson, arXiv Author ID - PubMed Author ID - Open ID) and CVU 2nd coauthor: (Scholar or SNI) (No.10 Times New Roman)

ID 3rd Coauthor: (ORC ID - Researcher ID Thomson, arXiv Author ID - PubMed Author ID - Open ID) and CVU 3rd coauthor: (Scholar or SNI) (No.10 Times New Roman)

(Report Submission Date: Month, Day, and Year); Accepted (Insert date of Acceptance: Use Only ECORFAN)

Abstract (In English, 150-200 words)

Objectives
Methodology
Contribution

Keywords (In English)

Indicate 3 keywords in Times New Roman and Bold No. 10

Abstract (In Spanish, 150-200 words)

Objectives
Methodology
Contribution

Keywords (In Spanish)

Indicate 3 keywords in Times New Roman and Bold No. 10

Citation: Surname (IN UPPERCASE), Name 1st Author, Surname (IN UPPERCASE), Name 1st Coauthor, Surname (IN UPPERCASE), Name 2nd Coauthor and Surname (IN UPPERCASE), Name 3rd Coauthor. Paper Title. Journal of Physiotherapy and Medical Technology. Year 1-1: 1-11 [Times New Roman No.10]

* Correspondence to Author (example@example.org)
† Researcher contributing as first author.

Introduction

Text in Times New Roman No.12, single space.

General explanation of the subject and explain why it is important.

What is your added value with respect to other techniques?

Clearly focus each of its features

Clearly explain the problem to be solved and the central hypothesis.

Explanation of sections Article.

Development of headings and subheadings of the article with subsequent numbers

[Title No.12 in Times New Roman, single spaced and bold]

Products in development No.12 Times New Roman, single spaced.

Including graphs, figures and tables-Editable

In the article content any graphic, table and figure should be editable formats that can change size, type and number of letter, for the purposes of edition, these must be high quality, not pixelated and should be noticeable even reducing image scale.

[Indicating the title at the bottom with No.10 and Times New Roman Bold]

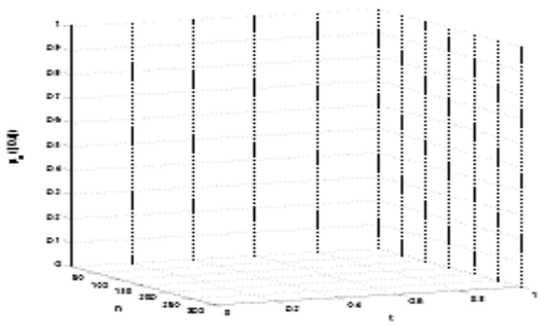

Graphic 1 Title and *Source (in italics)*

Should not be images-everything must be editable.

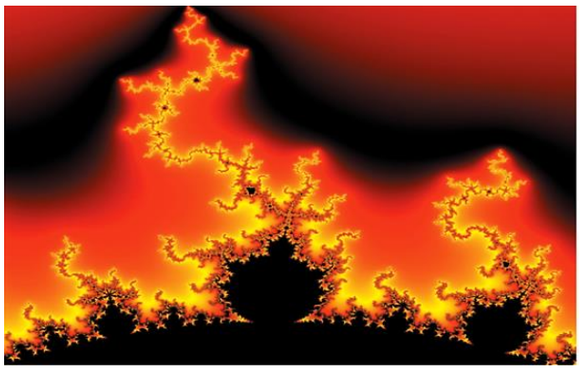

Figure 1 Title and *Source (in italics)*
Should not be images-everything must be editable.

Table 1 Title and *Source (in italics)*

Should not be images-everything must be editable.

Each article shall present separately in **3 folders**: a) Figures, b) Charts and c) Tables in .JPG format, indicating the number and sequential Bold Title.

For the use of equations, noted as follows:

$$Y_{ij} = \alpha + \sum_{h=1}^{r} \beta_h X_{hij} + u_j + e_{ij} \quad (1)$$

Must be editable and number aligned on the right side.

Methodology

Develop give the meaning of the variables in linear writing and important is the comparison of the used criteria.

Results

The results shall be by section of the article.

Annexes

Tables and adequate sources

Thanks

Indicate if they were financed by any institution, University or company.

ISSN 2523-6849

Conclusions

Explain clearly the results and possibilities of improvement.

References

Use APA system. Should not be numbered, nor with bullets, however if necessary numbering will be because reference or mention is made somewhere in the Article.

Use Roman Alphabet, all references you have used must be in the Roman Alphabet, even if you have quoted an Article, book in any of the official languages of the United Nations (English, French, German, Chinese, Russian, Portuguese, Italian, Spanish, Arabic), you must write the reference in Roman script and not in any of the official languages.

Technical Specifications

Each article must submit your dates into a Word document (.docx):

Journal Name
Article title
Abstract
Keywords
Article sections, for example:

1. Introduction
2. Description of the method
3. Analysis from the regression demand curve
4. Results
5. Thanks
6. Conclusions
7. References

Author Name (s)
Email Correspondence to Author
References

Intellectual Property Requirements for editing:

- Authentic Signature in Color of Originality Format Author and Coauthors.
- Authentic Signature in Color of the Acceptance Format of Author and Coauthors.
- Authentic Signature in blue color of the Conflict of Interest Format of Author and Co-authors.

ISSN 2523-6849

Reservation to Editorial Policy

Journal of Physiotherapy and Medical Technology reserves the right to make editorial changes required to adapt the Articles to the Editorial Policy of the Journal. Once the Article is accepted in its final version, the Journal will send the author the proofs for review. ECORFAN® will only accept the correction of errata and errors or omissions arising from the editing process of the Journal, reserving in full the copyrights and content dissemination. No deletions, substitutions or additions that alter the formation of the Article will be accepted.

Code of Ethics - Good Practices and Declaration of Solution to Editorial Conflicts

Declaration of Originality and unpublished character of the Article, of Authors, on the obtaining of data and interpretation of results, Acknowledgments, Conflict of interests, Assignment of rights and Distribution.

The ECORFAN-Mexico, S.C. Management claims to Authors of Articles that its content must be original, unpublished and of Scientific, Technological and Innovation content to be submitted for evaluation.

The Authors signing the Article must be the same that have contributed to its conception, realization and development, as well as obtaining the data, interpreting the results, drafting and reviewing it. The Corresponding Author of the proposed Article will request the form that follows.

Article title:

– The sending of an Article to Journal of Physiotherapy and Medical Technology emanates the commitment of the author not to submit it simultaneously to the consideration of other series publications for it must complement the Format of Originality for its Article, unless it is rejected by the Arbitration Committee, it may be withdrawn.

– None of the data presented in this article has been plagiarized or invented. The original data are clearly distinguished from those already published. And it is known of the test in PLAGSCAN if a level of plagiarism is detected Positive will not proceed to arbitrate.

– References are cited on which the information contained in the Article is based, as well as theories and data from other previously published Articles.

– The authors sign the Format of Authorization for their Article to be disseminated by means that ECORFAN-Mexico, S.C. In its Holding Taiwan considers pertinent for disclosure and diffusion of its Article its Rights of Work.

– Consent has been obtained from those who have contributed unpublished data obtained through verbal or written communication, and such communication and Authorship are adequately identified.

– The Author and Co-Authors who sign this work have participated in its planning, design and execution, as well as in the interpretation of the results. They also critically reviewed the paper, approved its final version and agreed with its publication.

– No signature responsible for the work has been omitted and the criteria of Scientific Authorization are satisfied.

– The results of this Article have been interpreted objectively. Any results contrary to the point of view of those who sign are exposed and discussed in the Article.

Copyright and Access

The publication of this Article supposes the transfer of the copyright to ECORFAN-Mexico, SC in its Holding Taiwan for its Journal of Physiotherapy and Medical Technology, which reserves the right to distribute on the Web the published version of the Article and the making available of the Article in This format supposes for its Authors the fulfilment of what is established in the Law of Science and Technology of the United Mexican States, regarding the obligation to allow access to the results of Scientific Research.

Article Title:

Name and Surnames of the Contact Author and the Co-authors	Signature
1.	
2.	
3.	
4.	

Principles of Ethics and Declaration of Solution to Editorial Conflicts

Editor Responsibilities

The Publisher undertakes to guarantee the confidentiality of the evaluation process, it may not disclose to the Arbitrators the identity of the Authors, nor may it reveal the identity of the Arbitrators at any time.

The Editor assumes the responsibility to properly inform the Author of the stage of the editorial process in which the text is sent, as well as the resolutions of Double-Blind Review.

The Editor should evaluate manuscripts and their intellectual content without distinction of race, gender, sexual orientation, religious beliefs, ethnicity, nationality, or the political philosophy of the Authors.

The Editor and his editing team of ECORFAN® Holdings will not disclose any information about Articles submitted to anyone other than the corresponding Author.

The Editor should make fair and impartial decisions and ensure a fair Double-Blind Review.

Responsibilities of the Editorial Board

The description of the peer review processes is made known by the Editorial Board in order that the Authors know what the evaluation criteria are and will always be willing to justify any controversy in the evaluation process. In case of Plagiarism Detection to the Article the Committee notifies the Authors for Violation to the Right of Scientific, Technological and Innovation Authorization.

Responsibilities of the Arbitration Committee

The Arbitrators undertake to notify about any unethical conduct by the Authors and to indicate all the information that may be reason to reject the publication of the Articles. In addition, they must undertake to keep confidential information related to the Articles they evaluate.

Any manuscript received for your arbitration must be treated as confidential, should not be displayed or discussed with other experts, except with the permission of the Editor.

The Arbitrators must be conducted objectively, any personal criticism of the Author is inappropriate.

The Arbitrators must express their points of view with clarity and with valid arguments that contribute to the Scientific, Technological and Innovation of the Author.

The Arbitrators should not evaluate manuscripts in which they have conflicts of interest and have been notified to the Editor before submitting the Article for Double-Blind Review.

Responsibilities of the Authors

Authors must guarantee that their articles are the product of their original work and that the data has been obtained ethically.

Authors must ensure that they have not been previously published or that they are not considered in another serial publication.

Authors must strictly follow the rules for the publication of Defined Articles by the Editorial Board.

The authors have requested that the text in all its forms be an unethical editorial behavior and is unacceptable, consequently, any manuscript that incurs in plagiarism is eliminated and not considered for publication.

Authors should cite publications that have been influential in the nature of the Article submitted to arbitration.

Information services

Indexation - Bases and Repositories

RESEARCH GATE (Germany)
GOOGLE SCHOLAR (Citation indices-Google)
MENDELEY (Bibliographic References Manager)
REDIB (Ibero-American Network of Innovation and Scientific Knowledge- CSIC)
HISPANA (Information and Bibliographic Orientation-Spain)

Publishing Services

Citation and Index Identification H
Management of Originality Format and Authorization
Testing Article with PLAGSCAN
Article Evaluation
Certificate of Double-Blind Review
Article Edition
Web layout
Indexing and Repository
ArticleTranslation
Article Publication
Certificate of Article
Service Billing

Editorial Policy and Management

69 Street. YongHe district, ZhongXin. Taipei - Taiwan. Phones: +52 1 55 6159 2296, +52 1 55 1260 0355, +52 1 55 6034 9181; Email: contact@ecorfan.org www.ecorfan.org

Journal of Physiotherapy and Medical Technology